A&A 507, 817–832 (2009)
DOI: 10.1051/0004-6361/200810925

Astronomy & Astrophysics

The stellar content of the Hamburg/ESO survey⋆

V. The metallicity distribution function of the Galactic halo

T. Schörck[1], N. Christlieb[2,3], J. G. Cohen[4], T. C. Beers[5], S. Shectman[6], I. Thompson[6], A. McWilliam[6], M. S. Bessell[7], J. E. Norris[7], J. Meléndez[8], S. Ramírez[9], D. Haynes[10], P. Cass[10], M. Hartley[10], K. Russell[10], F. Watson[10], F.-J. Zickgraf[1], B. Behnke[11], C. Fechner[12], B. Fuhrmeister[1], P. S. Barklem[3], B. Edvardsson[3], A. Frebel[13], L. Wisotzki[14], and D. Reimers[1]

(Affiliations can be found after the references)

Received 6 September 2008 / Accepted 7 September 2009

ABSTRACT

We determine the metallicity distribution function (MDF) of the Galactic halo by means of a sample of 1638 metal-poor stars selected from the Hamburg/ESO objective-prism survey (HES). The sample was corrected for minor biases introduced by the strategy for spectroscopic follow-up observations of the metal-poor candidates, namely "best and brightest stars first". Comparison of the metallicities [Fe/H] of the stars determined from moderate-resolution (i.e., $R \sim 2000$) follow-up spectra with results derived from abundance analyses based on high-resolution spectra (i.e., $R > 20\,000$) shows that the [Fe/H] estimates used for the determination of the halo MDF are accurate to within 0.3 dex, once highly C-rich stars are eliminated. We determined the selection function of the HES, which must be taken into account for a proper comparison between the HES MDF with MDFs of other stellar populations or those predicted by models of Galactic chemical evolution. The latter show a reasonable agreement with the overall shape of the HES MDF for [Fe/H] > -3.6, but only a model of Salvadori et al. (2007) with a critical metallicity for low-mass star formation of $Z_{\rm cr} = 10^{-3.4}\ Z_{\odot}$ reproduces the sharp drop at [Fe/H] ~ -3.6 present in the HES MDF. Although currently about ten stars at [Fe/H] < -3.6 are known, the evidence for the existence of a tail of the halo MDF extending to [Fe/H] ~ -5.5 is weak from the sample considered in this paper, because it only includes two stars [Fe/H] < -3.6. Therefore, a comparison with theoretical models has to await larger statistically complete and unbiased samples. A comparison of the MDF of Galactic globular clusters and of dSph satellites to the Galaxy shows qualitative agreement with the halo MDF, derived from the HES, once the selection function of the latter is included. However, statistical tests show that the differences between these are still highly significant.

Key words. stars: population II – surveys – Galaxy: evolution

1. Introduction

One of the key observables for constraining models of the formation and chemical evolution of the Galaxy is the Metallicity Distribution Function (MDF) of the constituent stars of its various components (bulge, disk, halo). The MDF provides critical information on the enrichment history of those components with heavy elements. In the case of the halo, early enrichment may have been provided by the very first generations of massive stars, formed from material of primordial composition shortly after the Big Bang (i.e., Population III stars).

Models of Galactic chemical evolution need to be compared to an accurate (and precise) observed halo MDF to test their predictions, to constrain their various parameters (such as the effective yield, the star-formation rate and the IMF), and in order to obtain information on the properties of Population III stars that are responsible for the earliest enrichment. This is particularly important for the lowest metallicity tail of the MDF, which provides invaluable information on the earliest enrichment phases (Prantzos 2003); for instance, it has been suggested that a minimum level of enrichment is required to form low-mass stars. This critical metallicity ranges between $10^{-4}\ Z_{\odot}$ (Omukai 2000; Bromm et al. 2001; Bromm & Loeb 2003; Umeda & Nomoto 2003; Santoro & Shull 2006; Frebel et al. 2007) and $10^{-6}\ Z_{\odot}$, the latter being applicable when dust grains are present (Schneider et al. 2002, 2003, 2006; Omukai et al. 2005; Tsuribe & Omukai 2006; Clark et al. 2008).

The precision of a derived halo MDF increases directly with the total number of observed metal-poor halo stars. Selection of such stars without the introduction of a kinematic bias (e.g., from among high proper motion stars) makes them of particular utility for examination of the relationships between the chemistry and kinematics of the halo. Early determinations of the halo MDF were based on small samples of globular clusters (Hartwick 1976; $N = 60$), or a mixture of halo subdwarfs and globular clusters (Bond 1981; $N = 90$ and $N = 31$, respectively). Problems with these samples arise not only from their small sizes, but also their inaccurate metallicities. Later studies employed significantly larger samples with spectroscopically-determined stellar abundances. For example, Ryan & Norris (1991) used a sample of 372 kinematically-selected halo stars. Ryan & Norris (1991) and Carney et al. (1996) showed that the MDF peaks at a metallicity of [Fe/H] $= -1.6$ with wings from [Fe/H] $= -3.0$ to solar abundances.

The HK survey (Beers et al. 1985, 1992; Beers 1999), originated by Preston and Shectman, and greatly extended by Beers to include several hundred additional objective-prism plates, was, until the advent of the Hamburg/ESO Survey (HES; see

⋆ Based on observations collected at Las Campanas Observatory, Palomar Observatory, Siding Spring Observatory, and the European Southern Observatory (Proposal IDs 69.D-0130, 170.D-0010, 073.D-0555, and 081.D-0596).

below), the primary source of metal-poor candidates suitable for consideration of the halo MDF. With the assistance of numerous colleagues, medium-resolution spectroscopy of over 10 000 HK-survey stars was obtained, using 1.5–4 m class telescopes, over the past two decades. This led to the identification of thousands of stars with [Fe/H] < −2.0, as well as significant numbers of stars with [Fe/H] < −3.0.

Another wide-angle spectroscopic survey is the HES. It was originally conceived as a survey for bright quasars (Reimers 1990; Wisotzki et al. 1996, 2000); however, its data quality is sufficient to not only efficiently select quasars with redshifts of up to $z = 3.2$, but also various types of stellar objects, including metal-poor stars (Christlieb et al. 2008). So far, several hundred new stars at [Fe/H] < −3.0 have been identified, including three stars that were confirmed by high-resolution spectroscopy to have [Fe/H] < −4.0: HE 1327−2326 ([Fe/H] = −5.4; Frebel et al. 2005; Aoki et al. 2006; Frebel et al. 2006a); HE 0107−5240 ([Fe/H] = −5.3; Christlieb et al. 2002, 2004; Bessell et al. 2004); and HE 0557−4840 ([Fe/H] = −4.8; Norris et al. 2007). It is perhaps of interest that the HK survey has not (to date) yielded any stars with [Fe/H] < −4.0 confirmed by high-resolution spectroscopy; this may be related to the fact that the HK survey reaches apparent magnitudes that are brighter than the HES, and as a result is dominated more than the HES by inner-halo stars.

The Sloan Digital Sky Survey (SDSS; Gunn et al. 1998; York et al. 2000), and in particular the Sloan Extension for Galactic Understanding and Exploration (SEGUE), has provided even larger samples of halo stars, as discussed by Carollo et al. (2007) and Ivezic et al. (2008). The former emphasize the division of the halo into two structural components, an inner region with $R < 10$–15 kpc, and an outer region beyond that radius. These two components differ in stellar metallicities, stellar orbits, and spatial density profiles. As we discuss in Sect. 2 below, the HES sample is dominated by inner-halo stars. We note that we hereafter refer to the inner halo as "the halo", unless indicated otherwise.

In spite of the very large sample of ∼20 000 stars used by Carollo et al., their coverage of the regime of very low metallicity is limited. According to their supplemental Fig. 4, they find only 3 stars with [Fe/H] < −3.0 in their "local sample" of 10 123 stars. The main reason for this is that the stars of their sample were not selected to be metal-poor, but for the purpose of spectrophotometric and telluric calibration of the SDSS spectra.

Recent high-resolution spectroscopic follow-up of stars from the Carollo et al. sample (Aoki, priv. comm.) has indicated that the current version of the SEGUE Stellar Parameter Pipeline (SSPP; see Lee et al. 2008a,b; Allende Prieto et al. 2008) is somewhat conservative in the assignment of stellar metallicity estimates, in the sense that stars assigned [Fe/H] < −2.7 by the SSPP are in reality more metal-deficient, on average, by on the order of 0.3 dex. A recent examination of the numbers of stars from the SDSS/SEGUE survey, taking into account this offset, suggests that up to several hundred stars with [Fe/H] < −3.0 are in fact present in the current SDSS sample of stars (including other categories of targets than just the calibration stars).

Ivezic et al. (2008) focus on the comparison between the inner halo and the disk. Since they rely on abundances determined from photometry, they cannot reliably determine metallicities of stars at [Fe/H] < −2. Nevertheless, the metallicity map of some 2.5 million stars with photometric metallicies shown in Fig. 8 of Ivezic et al. indicates that there exist very large numbers of stars in SDSS consistent with [Fe/H] < −2.0. Follow-up spectroscopy is, at present, only available for a subset of them. Beers et al. (in preparation) discuss the MDF of the lowest metallicity stars found in SDSS/SEGUE. The total number of stars with [Fe/H] < −2.0, based on medium-resolution SDSS spectroscopy, is over 25 000 (i.e., five times the number discovered by the combination of the HK and HES).

This paper continues our series on the stellar content of the HES (Christlieb et al. 2001b, Paper I; Christlieb et al. 2001a, Paper II; Christlieb et al. 2005, Paper III; Christlieb et al. 2008, Paper IV). We are mainly concerned with the low-metallicity tail of the halo MDF, which is constructed from a sample of 1638 metal-poor stars selected in the HES by quantitative criteria (Sect. 2). The follow-up observations and determination of the metallicities are described in Sect. 3. In Sect. 4 we detail how the MDF was constructed. We discuss the shape of the halo MDF in Sect. 5. Comparisons of the observed MDF with MDFs predicted by models of Galactic chemical evolution are presented in Sect. 6, and a comparison with the MDFs of the Galactic globular cluster system and dwarf spheroidal galaxies is presented in Sect. 7. The results are discussed in Sect. 8.

2. The metal-poor star sample

One of the main advantages of the HES for determining the halo MDF is that the selection of candidate metal-poor stars was done with quantitative criteria. Hence, the selection is well-understood, and possible selection biases can be quantified and corrected for during the construction of the MDF. Futhermore, the selection is purely spectroscopic, so it does not introduce any kinematic biases.

The selection of candidates in the HES is described in Paper IV. For the sample used in this study, we employed only the KP/$(B-V)_0$ selection; i.e., a star is selected as a metal-poor candidate if its KP index of the Ca II K line, as measured in its digital HES objective-prism spectrum, is smaller than the KP index predicted for a star of [Fe/H] = −2.5 and the same $(B-V)_0$ colour (see Fig. 5 of Paper IV). This cutoff was chosen because it results in a good compromise between completeness at [Fe/H] < −3.0, the region in [Fe/H] we are mainly interested in (because it corresponds to the earliest phases of Galactic chemical evolution), and achieving a selection that efficiently rejects stars at higher metallicity. In addition to the KP index, the $B-V$ colours are measured in the HES spectra as well (see Paper IV for details), and then are corrected for reddening using the maps of Schlegel et al. (1998). We restrict the sample to the colour range $0.5 < (B-V)_0 < 1.0$, because the follow-up observations of stars bluer than $(B-V)_0 = 0.5$ have not yet reached a sufficient level of completeness, and for stars redder than $(B-V)_0 = 1.0$, the accuracy of the determination of [Fe/H] from moderate-resolution follow-up spectra is limited due to the lack of calibration stars and the weakness of the Hδ line, which is used as a temperature indicator. The V magnitude and $(B-V)_0$ distribution of our sample together with isochrones for an age of 12 Gyr and different metallicities is shown in Fig. 1. The V magnitudes as well as the $(B-V)_0$ colours are from the HES.

The selection was applied to all spectra of unsaturated point sources extracted on 329 (out of 379) HES plates, covering a nominal area of ∼7700 deg^2 of the southern high galactic latitude sky. The candidates were visually inspected and assigned to the classes `mpca`, `unid`, `mpcb`, and `mpcc`. As described in Paper IV, the classification is based on the appearance of the Ca II K line in the digital HES spectra. Candidates of class `mpca` are the best in terms of the success rate of finding stars at [Fe/H] < −2.5 (see Fig. 8), since no Ca II K line could be

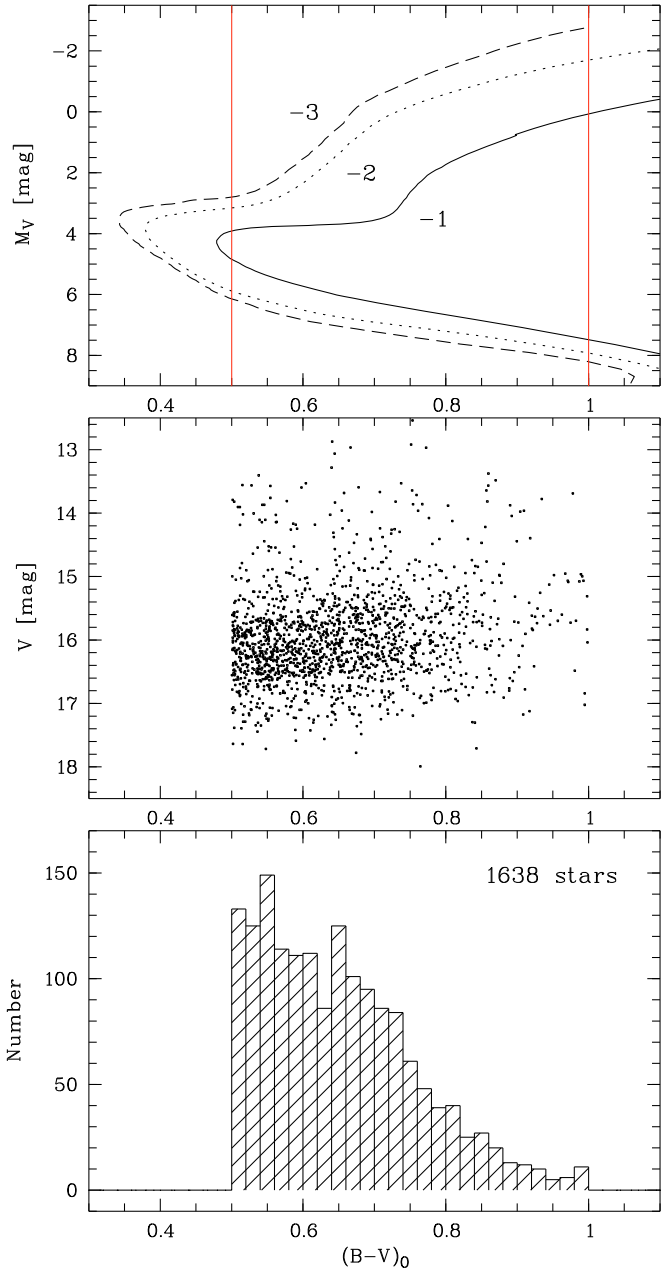

Fig. 1. *Upper panel*: isochrones for an age of 12 Gyr and metallicities of [Fe/H] = −1 to −3 (Kim et al. 2002), and chosen colour cuts (see text for details); *middle panel*: V magnitude distribution of the HES sample from which we construct the halo MDF; *lower panel*: $(B-V)_0$ distribution.

seen in the HES spectrum, while the candidates of class `mpcc` are the worst, because a strong Ca K line could clearly be seen. However, the Ca K line is still strong in cool, moderately metal-poor (i.e., [Fe/H] ∼ −2.0) giants, therefore the line is expected to be detected in the HES spectra of such stars. For statistical studies such as the determination of the halo MDF it is therefore necessary to obtain follow-up spectroscopy also of the `mpcc` candidates, because otherwise a color-related bias would be introduced. Furthermore, the assignment of classes to the candidates is subjective, and therefore it would be impossible to determine the selection function of the HES if only a subset of the candidates selected by quantitative criteria would be considered for the construction of the MDF.

Table 1. Number of stars in each candidate class.

Class	Number of stars			Factor
	all	observed	accepted	
`mpca`	201	123	105	1.63
`unid`	231	208	192	1.11
`mpcb`	2006	1008	940	1.99
`mpcc`	1275	432	401	2.95
Sum	3713	1771	1638	

Number in the total sample of candidates, number of observed candidates, and number of accepted candidates after removal of emission line objects, "peculiar" objects (e.g., objects with continuous spectra) and all stars with a G-band index GP > 6 Å. In the last column, we list the scaling factors applied to the [Fe/H] histograms for each candidate class during the construction of the MDF (see Sect. 4).

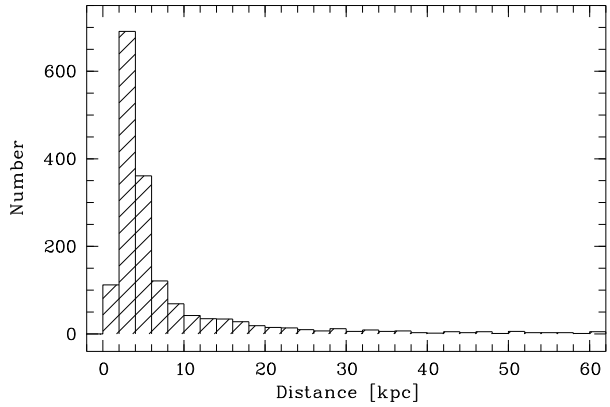

Fig. 2. Distance distribution of the HES sample. The sample is dominated by stars at distances of less than ∼5 kpc from the Sun; a few cool giants are located at distances of up to ∼50 kpc.

The result of the visual inspection are 3792 accepted candidates, of which 79 are present on multiple plate quarters or plates; the number of unique candidates is 3713. The number of candidates in each of the aforementioned classes is listed in Table 1. Only about half of the 3713 candidates are part of the sample presented in Table A.1 of Paper IV. This is because slightly improved sky background and spectrum extraction algorithms were used in the final reduction of the HES, from which the sample of Paper IV was drawn. While minor changes of the reduction algorithms can have a large effect on the measurement of the KP index in individual spectra, because the Ca II K line is covered by only four pixels of the HES spectra, we verified (HES plate by HES plate) that there are no systematic differences between the KP indices measured in spectra reduced with the older extraction algorithms and the spectra to which the selection described in Paper IV was applied. Therefore, there should not be any *statistical* differences between the HES metal-poor sample presented in Paper IV and the sample used in this paper. We decided to construct the halo MDF from an older sample because the spectroscopic follow-up observations of that sample is more advanced, resulting in a considerably larger sample size.

We determine distances to each of the sample stars using the [Fe/H] for each star and a set of isochrones similar to those shown in the upper panel of Fig. 1. Assuming that all the sample stars are at or above the main-sequence turnoff, we obtain the distance distribution shown in Fig. 2, and the spatial distribution shown in Fig. 3. The cooler giants in our sample reach distances from the Galactic plane well beyond $|Z| = 15$ kpc. However, the

Table 2. Follow-up observations of the candidate metal-poor stars.

Telescope(s)	Instrument(s)	Observers	N_{stars}
Magellan 1&2	B&C	Shectman, McWilliam, Thompson	553
SSO 2.3 m	DBS	Bessell, Norris, Edvardsson, Behnke, Christlieb, Frebel	339
Palomar 200"	DS	Cohen, Ramírez, Melendez	323
UK Schmidt	6dF	Haynes, Cass, Hartley, Russell, Watson	283
ESO 3.6 m	EFOSC2	Fechner, Zickgraf, Barklem, Fuhrmeister, Christlieb	140
Total			1638

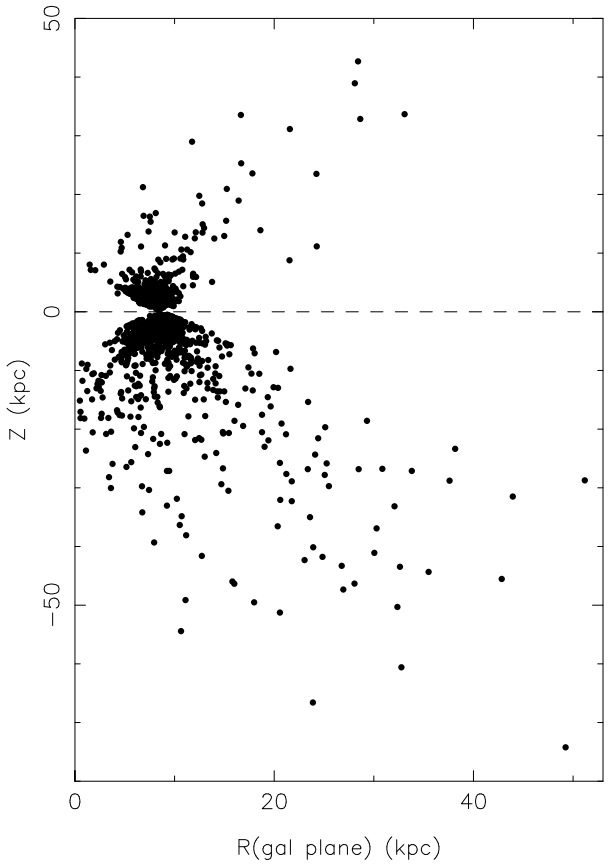

Fig. 3. Spatial distribution of the HES sample. R(gal.plane) is the distance from the Galactic center projected onto the Galactic plane.

sample is clearly dominated by inner-halo stars. There is a hint that the outer-halo stars with $|Z| > 15$ kpc have a higher fraction of extremely metal-poor stars than do those of the inner halo with $5 < |Z| < 15$ kpc, but given the wide range in metallicity we see throughout the halo, our sample is too small to determine the MDFs of the inner and outer halo separately with confidence.

3. Determination of metallicities

For 1771 of the 3713 unique candidates, moderate-resolution spectroscopy was obtained with various telescope/instrument combinations (see Table 2). The candidates were mostly observed in programs aiming at the identification of targets for high-resolution spectroscopy of the most metal-poor stars. Hence, the observing strategy adopted for the follow-up observations was to observe the brightest and best candidates (i.e., candidate classes `mpca` and `unid`) first.

In the follow-up spectra, we measured the KP index as well as the HP2 index of Hδ and the GP index for the G-band of CH (see Beers et al. 1999, for the definition of these indices). When multiple spectra for a star were available, the S/N-weighted average of the individual line index measurements was adopted. [Fe/H] was determined from the adopted HP2 and KP indices using the method of Beers et al. (1999). Since the publication of that paper, the algorithm was improved mainly by including more calibration stars, which results in better coverage of the relevant stellar parameter space, and in particular in a better coverage of the low-[Fe/H] region.

Since the stars of our sample were observed with many telescope/instrument combinations, it is important to verify that there are no systematic offsets between the measurements of the line indices in spectra taken at different telescopes. Such offsets could occur, for example, if the CCD response curves would strongly vary from instrument to instrument in the wavelength ranges in which the line and continuum bands of the indices are measured. For this reason, a number of candidate metal-poor stars were intentionally re-observed at different telescopes. Furthermore, in most of the observing campaigns, spectra of a few metal-poor standards (e.g., G 64−12, HD 140283, or CD −38° 245) as well as metal-poor radial-velocity standards were secured. In Fig. 4, we show comparisons of the KP and HP2 indices measured in spectra taken with all relevant telescope/instrument combinations. In total, 315 pairs of measurements are available. No systematic offsets between the measurements can be seen. However, the scatter of the measurements in spectra obtained with the UK Schmidt and the fibre-fed multi-object spectrograph 6dF are about a factor two larger than those of the other telescope/instrument combinations. This can be attributed to the fact that sky subtraction is more difficult for the 6dF spectra, since only a few fibers were dedicated to measure the sky background, and furthermore the sky brightness might have varied over the 6° diameter field of view of the instrument.

The quality of the spectra (i.e., $R \sim 2000$ and a typical S/N of 20 per pixel in the continuum near the Ca K line) allowed the easy identification and rejection of emission-line and other "peculiar" objects (e.g., galaxies, or objects with continuous spectra, such as cool, helium-rich white dwarfs). It has been shown by Cohen et al. (2005) that CH lines present in the continuum bands of the KP and HP2 indices lead to a systematic underestimation of these indices, resulting in systematically too low [Fe/H] values. Hence, we also excluded from this study all stars with GP > 6 Å. Since the fraction of carbon-enhanced stars among metal-poor stars increases as the metallicity decreases (see, e.g., Cohen et al. 2005; Lucatello et al. 2006), the rejection of stars with strong G-bands might lead to a bias against low-metallicity stars. However, since only 90 stars, or 5% of the 1771 observed stars, were rejected due to this reason, the

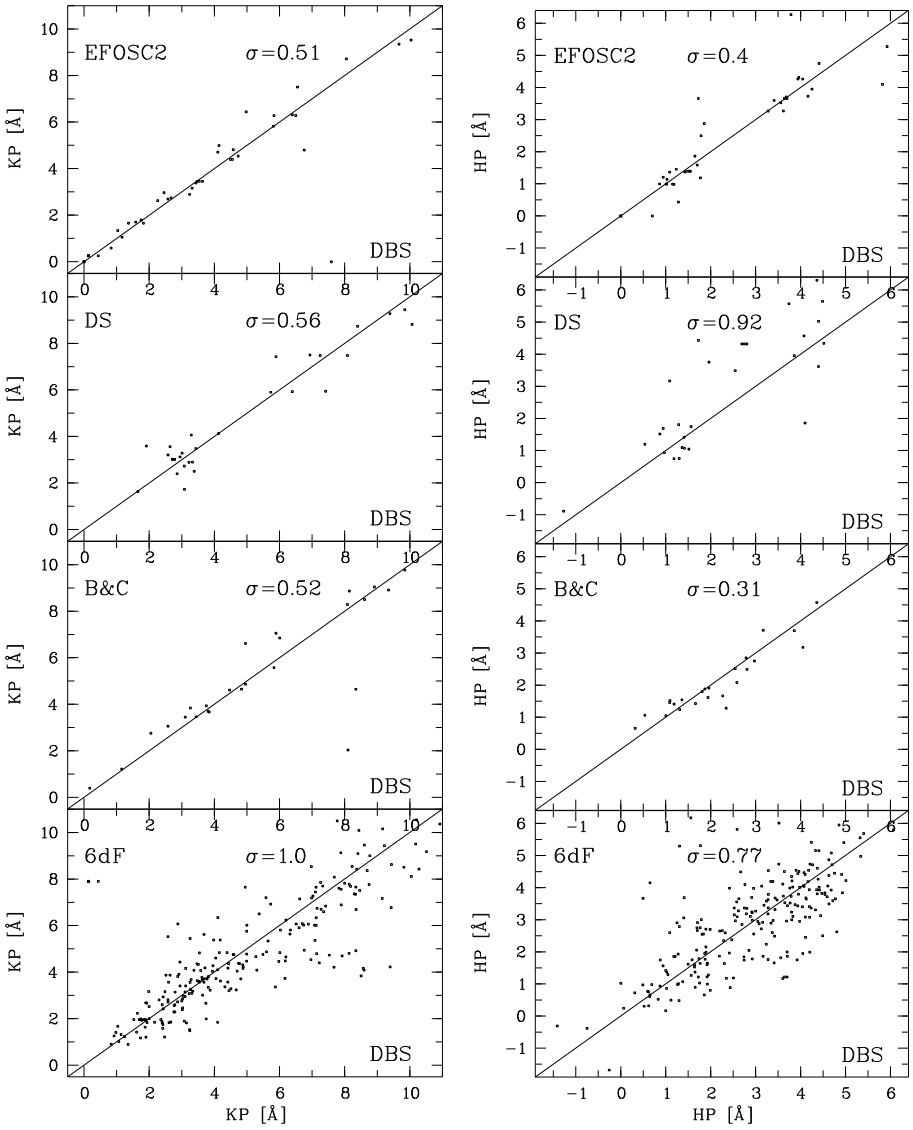

Fig. 4. Pairs of KP and HP2 measurements for the same star in spectra obtained with different telescope/instrument combinations. Note that some of the estimates of σ displayed in the panels are influenced by a number of outliers; i.e., robust estimates would yield smaller values.

possible effect on our sample is only minor. We also note that the three currently-known ultra metal-poor stars (i.e., stars with [Fe/H] < −4.0; see Sect. 4 below), all of which have large overabundances of carbon, are not rejected by this criterion, since their GP indices are smaller than 6 Å. In total, 133 stars were rejected, leaving 1638.

Homogeneous abundance analyses based on high-resolution spectra are available for 112 of the confirmed candidates in our sample. The spectra were taken with VLT/UVES (87 stars), Keck/HIRES (23 stars) or Magellan/MIKE (2 stars). The abundance analyses were performed by Barklem et al. (2005), Cohen et al. (2004), Cohen et al. (2006), Cohen et al. (2008), and Cohen (unpublished). Figure 5 compares the iron abundances determined in the course of these analyses ($[Fe/H]_{high-res}$) to the moderate-resolution follow-up results ($[Fe/H]_{med-res}$). No significant trends or offsets are present, and the 1-σ scatter around a regression line of the combined test sample is 0.3 dex. We hence conclude that the accuracy of $[Fe/H]_{med-res}$ for our sample is ±0.3 dex. We note that the accuracy can be increased especially for the cooler stars by using CCD photometry rather than $B - V$ colors predicted from the Hδ index HP2 when deriving $[Fe/H]_{med-res}$. However, CCD photometry is not yet available for all stars of our sample.

To increase the accuracy of the determination of the shape of the low-metallicity tail of the MDF, we replaced $[Fe/H]_{med-res}$ with $[Fe/H]_{high-res}$, where available. $[Fe/H]_{high-res}$ values are available for 27 of the 76 stars at $[Fe/H]_{med-res} < -3.0$, and five out of the six with $[Fe/H]_{med-res} < -3.5$. The $[Fe/H]_{high-res}$ values were taken from the references above and from Cayrel et al. (2004) for HE 0305−5442, a re-discovery of CS 22968-014 ($[Fe/H]_{high-res} = -3.56$). The sixth star at $[Fe/H]_{med-res} < -3.5$ in our sample for which a $[Fe/H]_{high-res}$ estimate is available has $[Fe/H]_{med-res} = -4.2$. A VLT/UVES spectrum exists for this star, and a preliminary abundance analysis confirms that the star has a metallicity close to or slightly below [Fe/H] = −4.0. Due to the preliminary nature of this result, we do not show this data point in Fig. 5.

4. Construction of the observed MDF

In order to investigate potential selection biases given the adopted follow-up observation strategy, it is instructive to compare the MDFs derived from stars of the individual candidate classes and in different magnitude ranges. For the purpose of investigating the possible presence of a bias caused by the fact that the brightest stars were observed first, we divided the full

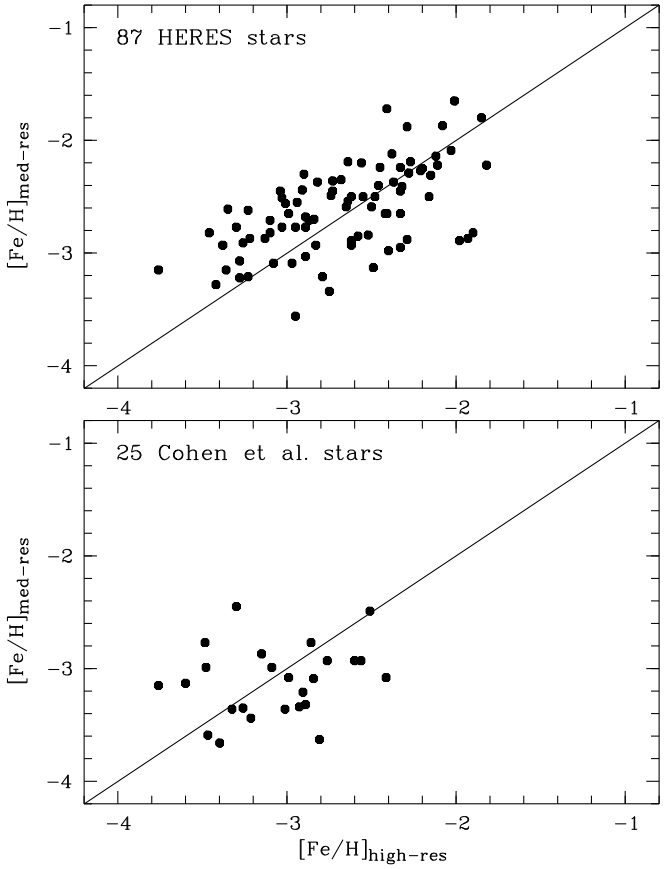

Fig. 5. Comparison of determinations of [Fe/H] from moderate-resolution follow-up spectra with results based on high-resolution spectroscopy. *Upper panel*: 87 stars observed with VLT/UVES (Barklem et al. 2005). *Lower panel*: 23 stars observed with Keck/HIRES and two with Magellan/MIKE; analyses carried out by Cohen et al. (2004), Cohen et al. (2006), Cohen et al. (2008), and Cohen (2008, unpublished).

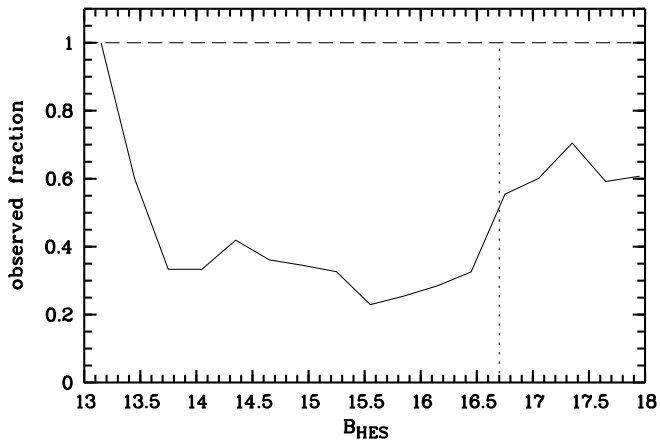

Fig. 6. Fraction of the stars in the HES sample for which moderate-resolution follow-up spectroscopy exists as function of B magnitude.

HES sample, as well as the subsamples of the four candidate classes, into a bright ($B \leq 16.7$) and a faint ($B > 16.7$) half, respectively. The results are shown in Fig. 7.

In the upper right panel it can be seen that the faint candidates are over-represented in the class `unid`. The reason is that the visual classification for fainter candidates, which have lower quality HES spectra, was more difficult. The bright- and faint-star [Fe/H] distributions of the other candidate classes, as well as the total sample, appear very similar to one another. This is quantitatively confirmed for the `mpca` and `unid` subsets by means of a Kolmogorov-Smirnov (KS) test of the null hypothesis H_0 that the bright and faint subsets of the stars belonging to these candidate classes were drawn from the same parent distribution, against the alternative hypothesis H_1 that they were not drawn from the same parent distribution. We chose a significance level of $\alpha = 0.01$; i.e., H_0 is rejected if the probability p of occurence of the test statistic (i.e., in case of the KS-test, D, the maximum distance between the cumulative probability distributions of the two samples), given H_0, is smaller than 0.01. The result of the KS-test for the bright and faint stars of the classes `mpca` and `unid` are $p = 0.82$ and $p = 0.21$, respectively; i.e., H_0 can clearly not be rejected in these cases. However, for the other two classes, the probabilities are considerably lower, ranging from 0.0046 (`mpcb`) to 0.073 (`mpcc`). For the full sample (i.e., all candidate classes combined), the probability is 0.0028; that is, the distributions of the bright and faint subsamples differ significantly from each other. It would hence be desirable to construct the halo MDF from the bright and faint samples separately. However, in this case the sample sizes would be too small to draw any conclusions, in particular about the low-metallicity tail of the MDF. Therefore, we decided to construct the halo MDF from the full sample. We note that the relative fraction of observed stars does not exhibit any strong biases towards bright or faint stars (see Fig. 6), thus the sample from which we construct the MDF should at least be representative for halo stars in the magnitude range $13 < B < 17.5$.

As can be seen in Fig. 8, the fraction of stars at [Fe/H] < -3.0 is highest among the `mpca` candidates (i.e., 7%), and significantly lower in the other classes (i.e., 3–4%). That is, the MDF of `mpca` candidates is biased towards lower metallicities. KS-tests show that the null hypotheses H_0 that subsamples of different candidate classes were drawn from the same parent distribution can clearly not be rejected for neighbouring classes (e.g., $p = 0.34$ for `unid` versus `mpcb`), while H_0 can be rejected at high significance when more distant classes are compared to each other (e.g., $p = 1.7 \times 10^{-5}$ for `mpca` versus `mpcc`). These tests and the bias of the candidates of class `mpca` towards low metallicity demonstrate that the candidate classification effectively separated the "good" from "bad" candidates. Figure 8 also shows that the number of false positives (i.e., stars at [Fe/H] > -2.5) is considerably higher among the `mpcc` candidates. However, this contamination does not affect our study, because we are mainly concerned with the low-metallicity tail of the MDF.

In order to properly take into account the stars of our candidate sample for which no spectroscopic follow-up observations exist, we constructed MDFs from the observed sample of stars in the following two ways. First, we computed separate MDFs for each of the candidate classes and scaled them such that the correct relative fraction of stars is produced when the four scaled MDFs are coadded; i.e., the scaling factors listed in the last column of Table 1 were applied. Secondly, we assigned to each of the 1942 stars in the full candidate sample lacking follow-up observations the [Fe/H] of a randomly selected star of the same candidate class for which a follow-up spectrum *is* available. We also randomly rejected stars with a too strong G-band and "peculiar" stars according to the probabilities determined from the

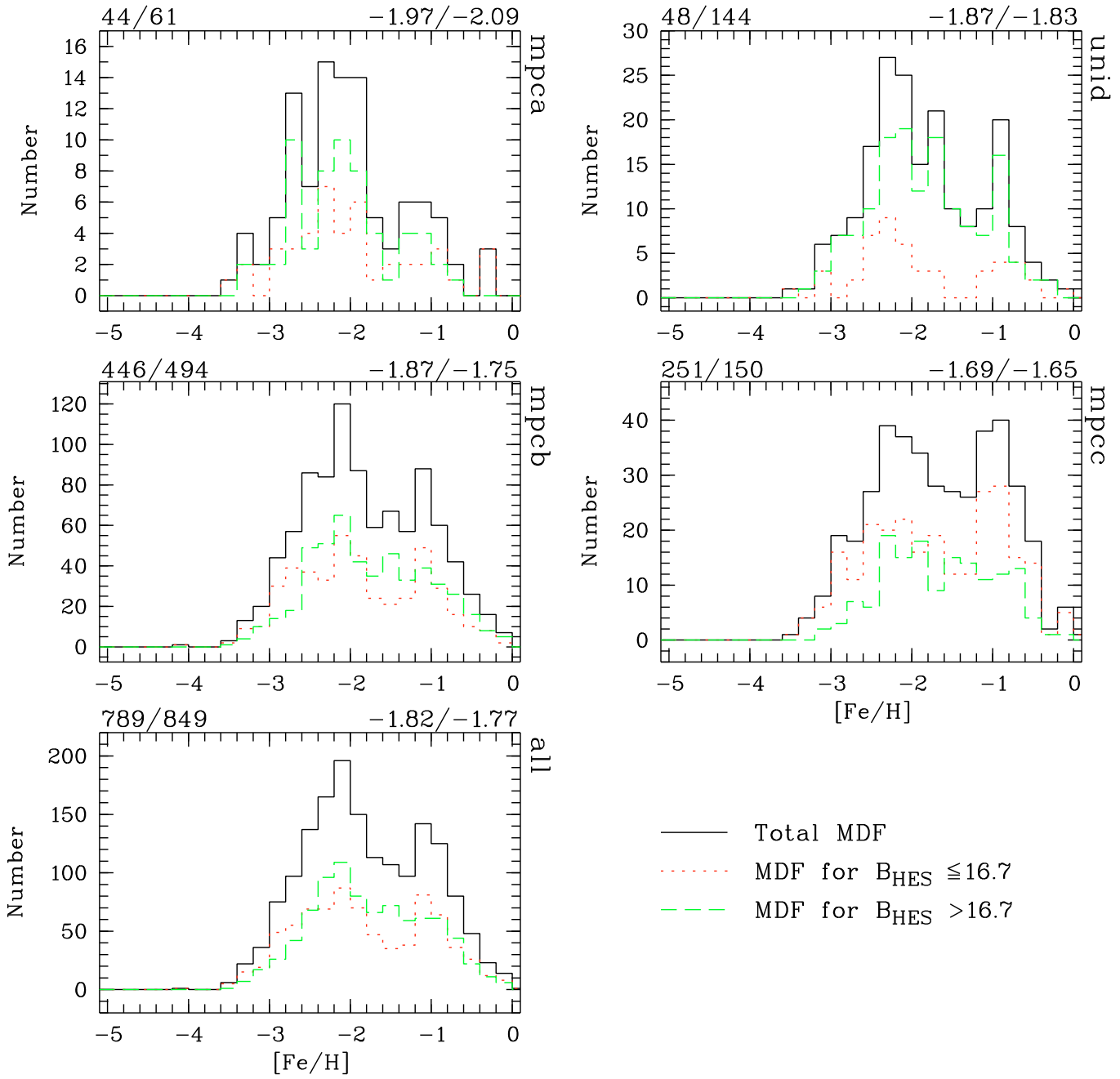

Fig. 7. Comparison of the MDFs of the bright ($B \leq 16.7$) and faint ($B > 16.7$) subsamples for each of the four candidate classes (*upper four panels*) as well as for the combined candidate sample (*lower left panel*). At *the top left* of each panel, the number of candidates belonging to the bright and faint sample, respectively, is listed; at *the top right*, the mean [Fe/H] of the samples is given.

sample for which follow-up observations exist. In this way, a sample of 3439 stars with the correct relative fraction of the candidates of the four classes was created.

The MDFs produced by these two methods are expected to be very similar to each other, because in each of them, the class-wise MDFs are scaled and then added to produce the final MDF; only the scaling methods are slightly different. Indeed, as can be seen in Fig. 9, the results do not differ significantly from each other. A χ^2-test of the null hypotheses H_0 that the two samples are drawn from the same distribution yields a probability of $p = 1.0$; i.e., H_0 can very clearly not be rejected. We adopt the MDF constructed by means of scaling the class-wise MDFs by a factor and adding them up. For this MDF, the numbers of stars in each metallicity bin are listed in Table 3.

Note that we have not corrected the MDF for the fact that as metallicity decreases, given that the giants become brighter and the dwarfs fainter (see Fig. 1), the relative volumes surveyed in our magnitude limited sample become larger and smaller, respectively. At $(B - V)_0 = 0.6$, for example, the data of the Yale-Yonsei isochrones (Kim et al. 2002) for an age of 12 Gyr suggest that the ratios of volume surveyed at [Fe/H] = −3 to that at [Fe/H] = −2 are 3.0 and 0.67 for giants and dwarfs, respectively. Due to the very small survey volume for dwarfs, no cool main-sequence star has so far been identified in the HES,

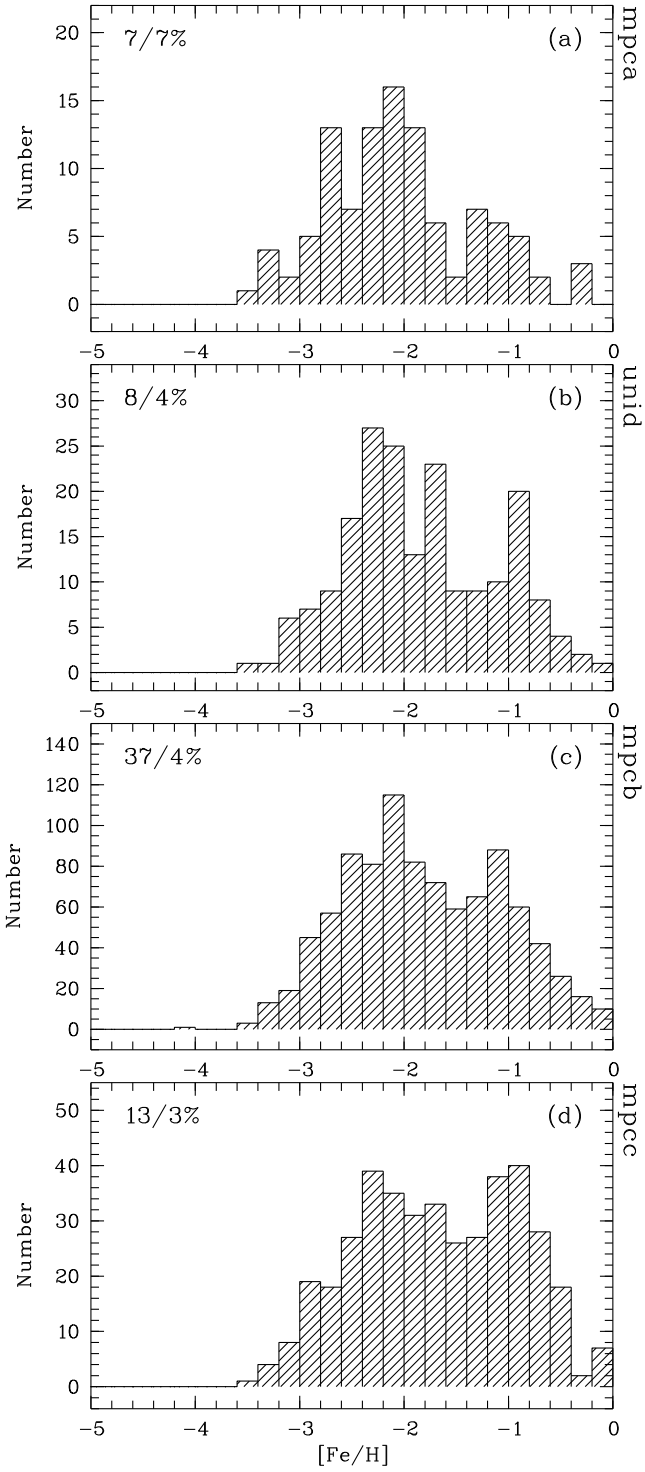

Fig. 8. Metallicity distribution of the HES sample of 1638 stars, divided by candidate class. In the upper left corner of each panel, the number of stars with [Fe/H] < −3.0 and the percentage of such stars within each candidate class is indicated.

and the sample considered in this paper is dominated by giants. Therefore, a survey volume correction would lead to a reduced relative number of stars at the lowest metallicities.

5. The shape of the halo MDF

A prominent feature in both of the scaled MDFs is a sharp drop at [Fe/H] ∼ −3.6 (see Fig. 9); in our (scaled) sample, only

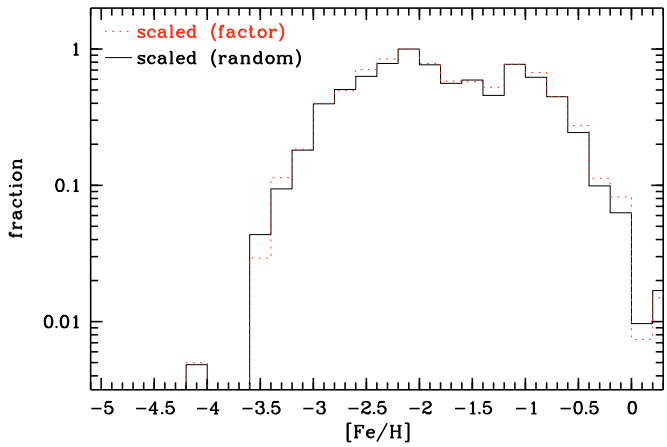

Fig. 9. Comparison of the MDFs constructed from the HES sample by means of random scaling and co-addition of the class-wise MDFs (solid black line) and scaling by factors (grey dotted line).

two out of 3439 stars have [Fe/H] < −3.6. Such a drop was also recognized by Norris (1999), and it has been seen in the Hamburg/ESO R-process Enhanced star Survey (HERES; see Fig. 2 of Barklem et al. 2005 and our Fig. 10). It reflects the fact that only very few stars at [Fe/H] < −3.6 were found in projects aiming at the identification and detailed study of the lowest metallicity stars of the Galactic halo, despite the considerable effort expended to find them (see, e.g., Cohen et al. 2008, and references therein).

The shape of the low-metallicity end of the halo MDF could not be determined precisely by Ryan & Norris (1991) due the limited size of their sample, which contains only four stars at [Fe/H] < −3.4, and none with [Fe/H] < −4.0. As can be seen in Fig. 11, in the range −3.4 < [Fe/H] < −2.5 their halo MDF agrees very well with the HES MDF. In Fig. 11 one can see a disagreement between the two MDFs in the bin centered on [Fe/H] = −3.5; i.e., the number of stars at this metallicity in the sample of Ryan & Norris is higher by about a factor of two as compared to the HES sample. Alternatively, the number of stars in the range −3.4 < [Fe/H] < −2.5 (i.e., the metallicity range which has been used to scale the two MDFs onto each other) are under-represented in the sample of Ryan & Norris, or over-represented in the HES sample. Even though the number of stars at [Fe/H] < −3.4 in both samples is small, the difference is significant. A KS-test of the null hypothesis H_0 that the HES sample and the sample of Ryan & Norris have the same parent distribution at [Fe/H] < −2.5 yields a probability of $p = 0.0087$; i.e., H_0 must (barely) be rejected if $\alpha = 0.01$ is chosen. The probability increases to 0.0091 if the two stars at [Fe/H] < −4.0 are excluded from the HES sample. The reason for the discrepancy is currently unclear, but one might speculate that it is related to the kinematic selection of the sample of Ryan & Norris and/or a larger fraction of stars belonging to the outer halo population being present in the HES sample.

Another feature of the halo MDF is a lightly populated tail extending to [Fe/H] < −5.0. The evidence for this feature from our (scaled) sample alone is weak, since it contains only two stars at [Fe/H] < −3.6, and none at [Fe/H] < −4.3. However, currently some ten stars with [Fe/H] < −3.6 have published abundance analyses based on high-resolution spectroscopy (see Table 4 of Beers & Christlieb 2005, for a recent review), including three additional stars at [Fe/H] < −4.0: HE 1327−2326 ([Fe/H] = −5.4; Frebel et al. 2005; Aoki et al. 2006;

Table 3. The MDF of the Galactic halo field stars as constructed from the sample of 1638 HES with available spectroscopic follow-up observations, by means of scaling to the full candidate sample of 3439 stars (for details see text).

[Fe/H]	−4.50	−4.30	−4.10	−3.90	−3.70	−3.50	−3.30	−3.10	−2.90	−2.70	−2.50	−2.30	−2.10
N	0	0	2	0	0	12	45	73	160	198	281	337	399
[Fe/H]	−1.90	−1.70	−1.50	−1.30	−1.10	−0.90	−0.70	−0.50	−0.30	−0.10	+0.10	+0.30	+0.50
N	313	231	229	209	308	268	178	109	45	33	3	6	0

Note that for a proper comparison with the MDFs predicted by theoretical models, or the MDFs of other stellar populations, the selection efficiency of the HES as a function of [Fe/H] and $(B-V)_0$ must be taken into account (see Table 4). Note also that the HES sample is increasingly contaminated with thin- and thick-disk stars as [Fe/H] approaches 0.0.

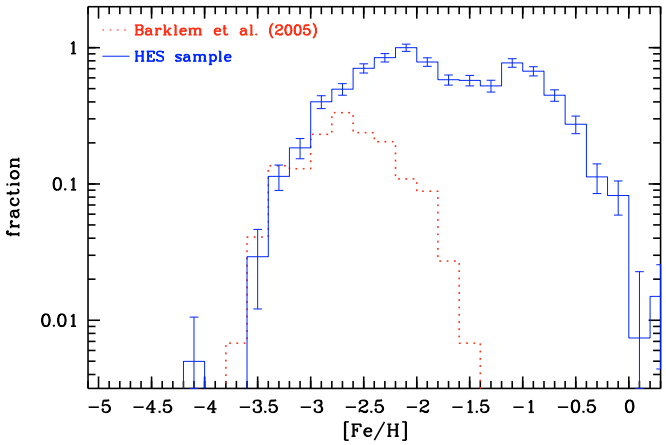

Fig. 10. Comparison of the MDF constructed from the HES sample (solid line) with that of the HERES sample analysed by Barklem et al. (2005, grey dotted line). The latter sample is biased against stars at [Fe/H] > −3.0, because most stars at higher metallicity were intentionally removed due to the science aims of that survey.

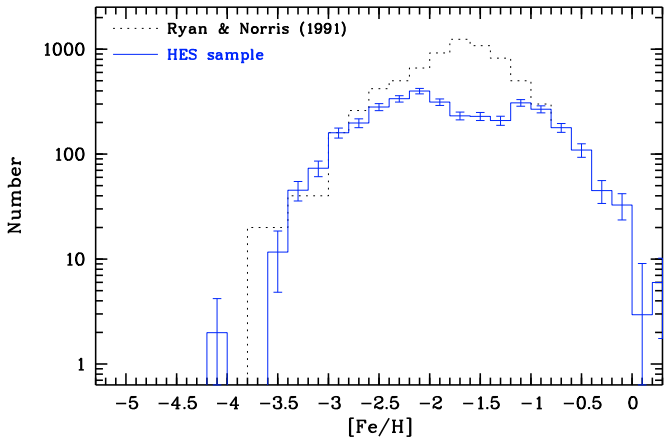

Fig. 11. Comparison of the halo MDF constructed from the HES sample (histogram) with that of Ryan & Norris (1991), scaled to match the HES MDF in the range −3.4 < [Fe/H] < −2.5 (dotted line).

Frebel et al. 2006a), HE 0107−5240 ([Fe/H] = −5.3; Christlieb et al. 2002, 2004; Bessell et al. 2004), and HE 0557−4840 ([Fe/H] = −4.8; Norris et al. 2007). These three stars are not part of our sample due to a variety of reasons. HE 1327−2326 is part of the bright HES metal-poor sample consisting of stars above a saturation threshold (Frebel et al. 2006b), while only unsaturated point sources entered the sample of this work. HE 0107−5240 was selected in a previous version of the candidate selection which was slightly less restrictive than the one we use here; as a result, this star misses the selection cutoff of 3.9 Å for its HES $(B-V)_0$ colour of 0.6 mag by 0.1 Å (i.e., the KP index measured in the HES spectrum is 4.0 Å). And finally, HE 0557−4840 is located on one of the 50 HES plates which are not considered here. In conclusion, for an accurate determination of the shape of the MDF at [Fe/H] < −4.0 it is required to compile even larger statistically complete samples of metal-poor stars.

6. Comparison between theoretical MDFs and the halo MDF

In a comparison of the observed MDF with MDFs predicted by theoretical models, one has to take into account the modification of the shape of the MDF by the selection of metal-poor candidates employed in the HES. In particular, uncertainties $\sigma_{\rm KP}$ and σ_{B-V} of the measurements of the KP index and $B-V$ in the HES spectra result in a scatter of stars with [Fe/H] > −2.5 into the sample, and stars with [Fe/H] < −2.5 out of the sample. Each theoretical MDF under investigation is therefore converted into an MDF as it would be observed in the HES, by applying the metal-poor star selection criteria used in the HES.

The first step in the conversion of a theoretical MDF is the simulation of a sample of stars with a distribution in [Fe/H] according to that of the theoretical MDF under investigation. The [Fe/H] values are then converted into pairs of KP and $(B-V)_0$ by inverting the calibrations of Beers et al. (1999). Then, a subsample was selected such that it follows the distribution in $(B-V)_0$ of the HES sample (see Fig. 1). Taking into account the distribution in $(B-V)_0$ is important because the shape of the selection function is determined by $\sigma_{\rm KP}$, σ_{B-V}, and the gradient of [Fe/H] in the KP versus $(B-V)_0$ parameter space (see Fig. 4 of Paper IV); it varies with $(B-V)_0$, as can be seen in Fig. 12.

The reader will note that we have excluded stars with $(B-V)_0 < 0.5$ from our sample, which in principle will affect the relative proportions of dwarfs admitted to our sample as a function of [Fe/H]. In practice, however, this is not a serious effect if we restrict our abundance range to abundances [Fe/H] < −2.0. Consideration of the Yale-Yonsei isochrones for an age of 12 Gyr, and for the Salpeter mass function ($x = 1.35$), shows that the percentages of dwarfs with $(B-V)_0 < 0.5$ relative to all main-sequence stars with mass greater that 0.40 $M_\odot$ are 4, 13, 19, 22, 24, and 24 for [Fe/H] = −1.0, −1,5, −2.0, −2.5, −3.0, and −3.5, respectively. That is to say, the proportion of excluded dwarfs is relatively constant for [Fe/H] < −2.0.

The next step in the procedure of converting theoretical MDFs into an MDF as it would be observed in the HES was to add random Gaussian errors with standard deviations according to the known measurement uncertainties $\sigma_{\rm KP}$, σ_{B-V} in the HES to KP and $(B-V)_0$ assigned to each star. Finally, the KP/$(B-V)_0$ selection criterion was applied to the simulated sample

Table 4. Selection function for HES metal-poor candidates in the colour range $0.5 < (B-V)_0 < 1.0$, as determined from a simulated sample of stars following the MDF predicted by the Simple Model of Galactic chemical evolution (Searle & Sargent 1972; Hartwick 1976).

[Fe/H]	Selected fraction at $(B-V)_0$					
	0.5	0.6	0.7	0.8	0.9	1.0
−4.05	1.000	1.000	1.000	1.000	1.000	1.000
−3.95	0.958	1.000	1.000	1.000	1.000	1.000
−3.85	1.000	0.962	1.000	1.000	1.000	1.000
−3.75	0.961	1.000	1.000	1.000	1.000	1.000
−3.65	0.982	0.987	1.000	1.000	1.000	1.000
−3.55	0.954	0.991	1.000	1.000	1.000	1.000
−3.45	0.920	0.991	0.997	0.996	1.000	1.000
−3.35	0.924	0.979	0.993	0.996	0.997	1.000
−3.25	0.901	0.976	0.989	0.991	0.985	1.000
−3.15	0.861	0.950	0.984	0.974	0.981	0.997
−3.05	0.816	0.919	0.958	0.954	0.953	0.983
−2.95	0.744	0.869	0.928	0.908	0.900	0.949
−2.85	0.668	0.801	0.879	0.852	0.839	0.918
−2.75	0.563	0.700	0.812	0.768	0.743	0.822
−2.65	0.455	0.583	0.715	0.658	0.617	0.709
−2.55	0.340	0.457	0.592	0.537	0.488	0.573
−2.45	0.232	0.337	0.462	0.406	0.364	0.433
−2.35	0.140	0.234	0.331	0.297	0.264	0.318
−2.25	0.075	0.149	0.222	0.203	0.187	0.217
−2.15	0.034	0.088	0.136	0.130	0.127	0.152
−2.05	0.013	0.046	0.079	0.081	0.085	0.100
−1.95	0.004	0.021	0.043	0.048	0.058	0.070
−1.85	0.001	0.009	0.022	0.028	0.041	0.051
−1.75	0.000	0.003	0.011	0.017	0.028	0.036
−1.65	0.000	0.001	0.006	0.010	0.020	0.028
−1.55	0.000	0.000	0.003	0.006	0.015	0.021
−1.45	0.000	0.000	0.001	0.004	0.010	0.017
−1.35	0.000	0.000	0.001	0.003	0.007	0.014
−1.25	0.000	0.000	0.001	0.002	0.004	0.008
−1.15	0.000	0.000	0.000	0.001	0.002	0.008
−1.05	0.000	0.000	0.000	0.001	0.001	0.004
−0.95	0.000	0.000	0.000	0.000	0.000	0.000
−0.85	0.000	0.000	0.000	0.000	0.000	0.000

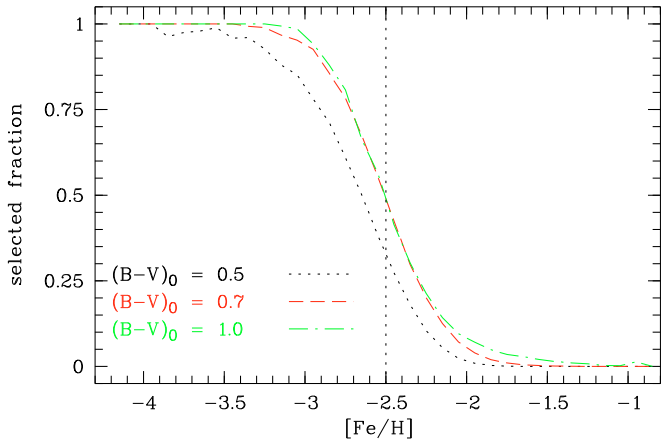

Fig. 12. Selection function for HES metal-poor candidates of $(B-V)_0 = 0.5$, 0.7, and 1.0, as determined from a simulated sample of stars following the MDF predicted by the Simple Model of Galactic chemical evolution (Searle & Sargent 1972; Hartwick 1976).

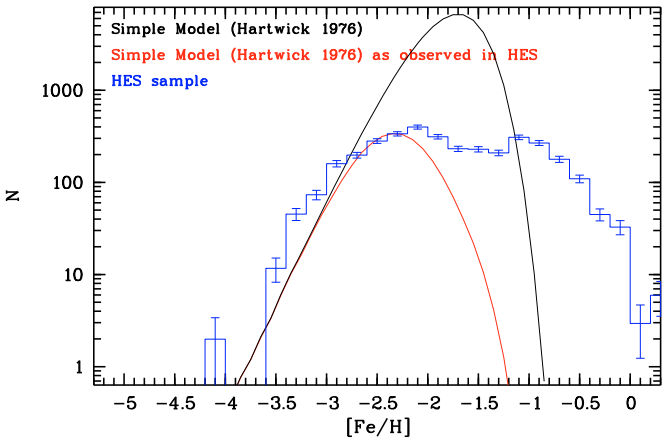

Fig. 13. Comparison of the MDF of a Simple Model with $y_{\rm eff} = -1.7$ (black line) with the MDF constructed from the HES sample (histogram). The grey line illustrates how the MDF of the Simple Model would be observed in the HES. For the comparison between the theoretical model and the observations, only the grey line in the metallicity range below [Fe/H] ~ -2.0 should be taken into account, because at higher [Fe/H] the HES sample is contaminated with thin- and thick-disk stars.

of stars. The [Fe/H] distribution of the selected stars is the MDF as it would be observed in the HES.

For the convenience of the reader, we list in Table 4 and show in Fig. 12 the HES metal-poor star selection function as determined with a simulated sample of stars following the MDF predicted by the Simple Model of Galactic chemical evolution (Searle & Sargent 1972; Hartwick 1976). That model assumes that a fiducial "closed box" of primordial gas is enriched by successive stellar generations. Further model assumptions are that (i) the gas is well-mixed at all times (i.e. there is a unique age-metallicity relation for the stars formed from that gas) and (ii) the stellar initial mass function (IMF) does not change with time. Analytical solutions can only be obtained if it is assumed that the evolutionary timescales of the enriching stars are neglible (the so-called Instantaneous Recycling Approximation or IRA). Such solutions can be generically obtained in the case of a closed box, and in some particular cases of outflow (gas loss from the box) and infall (gas flows into the box). Since the IRA turns out to be a very good approximation for elements ejected by massive stars, those analytical solutions can provide a powerful tool for the study of Galactic systems.

In the framework of the Simple Model, the shape of the MDF can be described in terms of a unique parameter, the "yield", which is the ratio of the mass of newly-created metals to the mass locked in long-lived stars and stellar remnants. This is a very useful parametrization, because it is independent of the star formation history of the system (the major unknown in Galactic evolution studies). In the closed box model the yield depends only on the IMF (referred to as the "true yield"), while in the case of gaseous flows (infall and outflow) it depends also on their magnitude; this "effective yield", $y_{\rm eff}$, is always smaller than the true yield. It turns out that the MDF peaks at a metallicity equal to the effective yield; this simple result allows one to determine the effective yield and to constrain the underlying physics (IMF, outflow rate, etc.).

In Fig. 13, we compare the MDF of a Simple Model with $y_{\rm eff} = -1.7$ with the MDF observed in the HES. The HES MDF shows an excess of stars in the range $-3.5 <$ [Fe/H] < -3.0. Alternatively, if the MDF of the Simple Model would be scaled such that it matches the observed MDF in this range, a large

deficit of the number of observed stars in the range $-3.0 <$ [Fe/H] < -2.0 with respect to the Simple Model would result. It is also neither possible to reproduce with the Simple Model the sharp drop of the observed MDF at [Fe/H] $= -3.6$, nor the tail at [Fe/H] < -3.6.

Prantzos (2003) developed a modification of the Simple Model, which includes early infall, and later outflow of gas; the IRA is also relaxed in his model. Prantzos (2007) suggested that since the halo of the Galaxy has been assembled by merging of a large number of fragments, the MDF of the Galactic halo can be seen as the sum of the MDFs of these fragments. In his model, the chemical evolution histories of each of the fragments are still described by the Simple Model, using the observed mass-metallicity relation of dwarf galaxies to derive individual effective yields. The halo MDF is then produced by integrating over a mass function of the fragments determined in numerical simulations. The MDFs of the models of (Prantzos 2003, 2007) are shown in Fig. 15. Both MDFs match the HES MDF well in the range $-3.5 <$ [Fe/H] < -2.5 and at [Fe/H] ~ -4.0, but the sharp drop at [Fe/H] ~ -3.6 is not predicted by them.

The next set of models that we consider are those of Salvadori et al. (2007), who reconstruct the merger tree of the Milky Way with a semi-analytic approach including a chemical evolution code. A free parameter in this model is the critical metallicity for low-mass star formation, $Z_{\rm cr}$. As can be seen in Fig. 14, the model with $Z_{\rm cr} = 10^{-3.4}\ Z_\odot$ reproduces the drop of the observed MDF at [Fe/H] ~ -3.6 rather well. However, the model predicts that no stars at [Fe/H] < -3.6 should exist, while there are two such stars in our sample, and for about ten additional stars in this metallicity range abundance analyses based on high-resolution spectroscopy have been published (see Table 4 of the review of Beers & Christlieb 2005).

The Salvadori et al. model with $Z_{\rm cr} = 10^{-4.0}\ Z_\odot$ matches the HES MDF at [Fe/H] ~ -4.0, but disagrees in the range $-4.0 <$ [Fe/H] < -3.6, where ~30–70 stars are predicted, but none are present in our sample. The model with $Z_{\rm cr} = 0$ over-predicts the number of stars in this metallicity range even more strongly, and it greatly over-predicts that number of stars at [Fe/H] < -4.0, as already discussed by Salvadori et al. (2007).

Finally, we compare in Fig. 16 the HES MDF with that predicted by the stochastic chemical enrichment model of Karlsson (2006). While the model matches the HES MDF at [Fe/H] ~ -4.0, and predicts the tail at [Fe/H] < -4.0 that is known to exist from additional stars published in the recent literature, the drop of the observed MDF at [Fe/H] ~ -3.6 is not present in the theoretical MDF.

To quantify our comparisons of the HES MDF with those predicted by the theoretical models discussed above, we carried out KS-tests of the null hypotheses H_0 that the HES sample and the individual samples simulated according to the MDFs of the models were drawn from the same parent distribution, at a significance level of $\alpha = 0.01$. The tests were restricted to [Fe/H] < -3.0, because we are mainly concerned with the shape of the low-metallicity tail of the MDF. The result of the tests are that H_0 can not be rejected ($p = 0.063$) only in the case of the Salvadori et al. model for $Z_{\rm cr} = 10^{-3.4}\ Z_\odot$. However, we note that the statistical test of Kuiper (1962), which according to Press et al. (1992) is more sensitive than the KS-test to differences at the ends of the two distributions under comparison (i.e., at the lowest and highest metallicities), yields $p = 6.5 \times 10^{-4}$; i.e., if this test is employed, H_0 would be rejected at high significance. All other models considered yielded $p < 10^{-3}$, regardless of which of the two tests were applied.

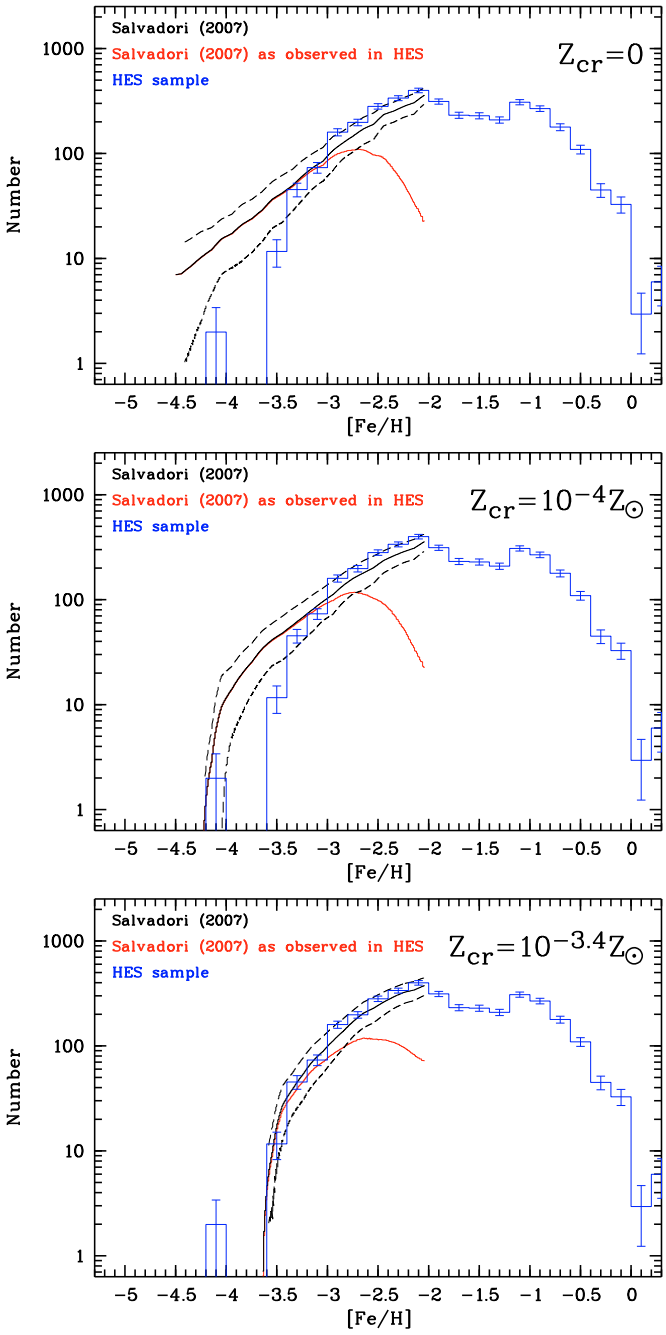

Fig. 14. Comparison of the MDF constructed from the HES sample (histogram) with models of Salvadori et al. (2007) with different critical metallicities $Z_{\rm cr}$ (black and grey lines). The region between the dashed lines indicates the uncertainty of the models due to different hierarchical merger histories of the Galaxy.

7. Comparison of the halo field star MDF with that of other stellar populations

It is of great interest to compare the halo MDF with the MDF found for other stellar populations, in particular for the system of Galactic globular clusters (hereafter GCs) and for the stars in dwarf spheroidal (dSph) galaxies. Since the most metal-poor Galactic GC has [Fe/H] ~ -2.5, we need to establish whether or not there is a real deficit of GCs at lower Fe-metallicities compared to the halo field.

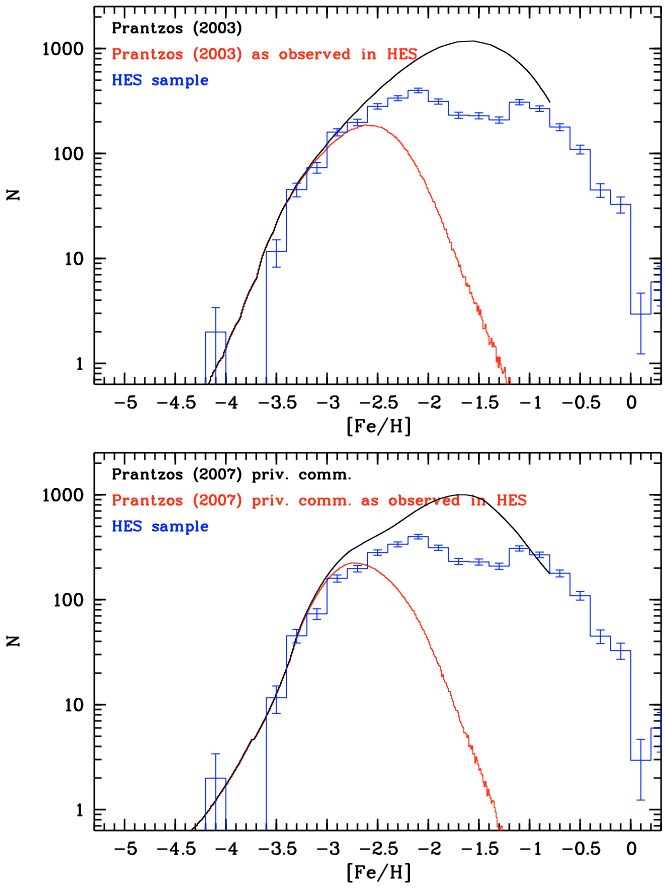

Fig. 15. Comparison of the MDF constructed from the HES sample (histogram) with theoretical predictions (black and grey lines). *Upper panel*: Prantzos (2003); *lower panel*: Prantzos (2007).

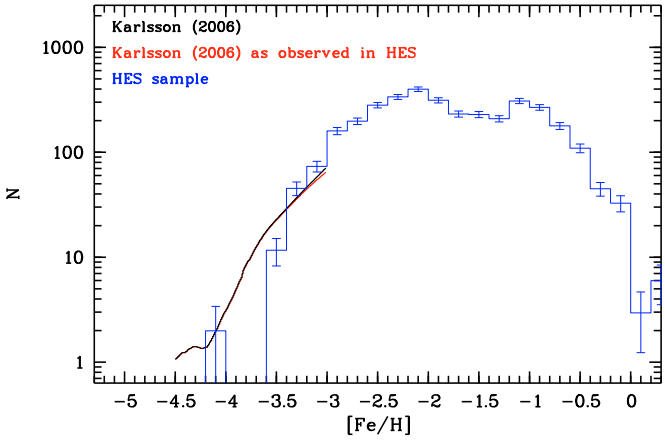

Fig. 16. Comparison of the halo MDF constructed from the HES sample with the MDF predicted by the stochastic chemical enrichment model of Karlsson (2006).

For a proper comparison of the HES MDF with that of other stellar populations, it is mandatory that the selection function of the HES, as listed in Table 4, be taken into account. The values in that table can be used to correct the observed MDF for the selection of metal-poor candidates employed in the HES. This is particularly important at [Fe/H] > -2.5, where the corrections are large, because typically less than half of the stars are actually picked up by the HES. Note that this incompleteness is intended, because the main aim of the search for metal-poor stars with the HES is to identify stars with [Fe/H] < -3.0. Therefore, the selection of candidate metal-poor stars was designed such that as many stars at [Fe/H] > -3.0 as possible are rejected, while maintaining a high degree of completeness at [Fe/H] < -3.0 (see Christlieb et al. 2008, for details).

For a star of a given [Fe/H], the corrections are also a function of $B - V$ color, being higher (more likely for a star to be included in the HES) for redder stars. The variation over the $B - V$ color range of the HES sample can, in extreme cases at the higher metallicities, correspond to a variation of a factor of 8 in selection efficiency (see, e.g., the line for [Fe/H] $= -1.95$ in Table 4).

For our comparison with the MDF of the Galactic GCs we adopt the [Fe/H] values from the current version of the online database of Harris (1996). The values for M15 and for NGC 7099 were updated with small corrections based on detailed abundance analyses carried out by Cohen and collaborators (Cohen & Huang, in preparation; Cohen et al., in preparation). The HES is (intentionally) incomplete for [Fe/H] > -2.0, so we only consider the set of GCs with [Fe/H] < -1.95, which contains only 16 clusters. We note that many analyses have shown that the Galactic GCs exhibit the same behaviour of abundance ratios (such as the increase of [Ca/Fe] with decreasing [Fe/H]) as the halo stars (e.g., Fig. 23 of Cohen et al. 2004) as do the halo stars. Thus, the conversion between a Ca line index and [Fe/H] adopted by the HES should be appropriate for Galactic GCs stars as well.

Figure 17 shows the cumulative MDF from the HES sample and for the Galactic GC system. The raw MDF and that corrected for the selection efficiency of the HES, given in Table 4, are shown. Note that the selection efficiency takes into account the uncertainties for [Fe/H] which result from the uncertainties of the measurement of KP and $(B - V)$ from HES spectra, which result in $\sigma_{[\mathrm{Fe/H}]}$ between 0.2 dex and 1.0 dex, depending on $(B - V)$ colour (Christlieb et al. 2008). Simulations suggest that for a sample with more accurate [Fe/H] determinations, such as the Galactic GCs, the maximum difference in the cumulative distribution up to [Fe/H] ~ -2.0 compared to that given in Table 4 is small and does not exceed the difference between the various corrected cumulative MDFs given in Cols. 3 to 5 of that table.

The solid, middle line in Fig. 17 corresponds to the case where corrections according to the dereddened $B - V$ color of each individual star of the HES sample have been applied. Since these corrections are themselves uncertain, two other variants are shown in this figure, and listed in Table 5, to indicate the potential impact of the choice of $B - V$ color on the corrections. The first adopts the corrections for the bluest $B - V$ color of Table 4, which are always the smallest, while the the second uses that of the reddest $B - V$ color of Table 4, which are always the largest.

Figure 17 shows that once the selection efficiency corrections given Table 4 are applied, the halo field star MDF we deduce here is a good match to that of the Galactic GCs. Instead of expecting roughly 10% of the sample covering the range [Fe/H] < -1.95 to have [Fe/H] < -3.0, we expect only ~2% to be this metal deficient, when the selection efficiency for the HES is taken into account. At [Fe/H] < -2.5, the expected fraction decreases from 50% to 8%. Thus, the absence of any GC more metal-poor than -2.5 dex among a sample of 16 clusters at [Fe/H] < -1.95 is not suprising.

A similar situation holds for the stellar population in the dSph satellites of the Galaxy. It has been widely claimed (see, e.g. the review by Geisler et al. 2007) that these dSph stellar populations show a significant lack of stars with Fe-metallicity at [Fe/H] < -3.0. For example, Helmi et al. (2006) make this

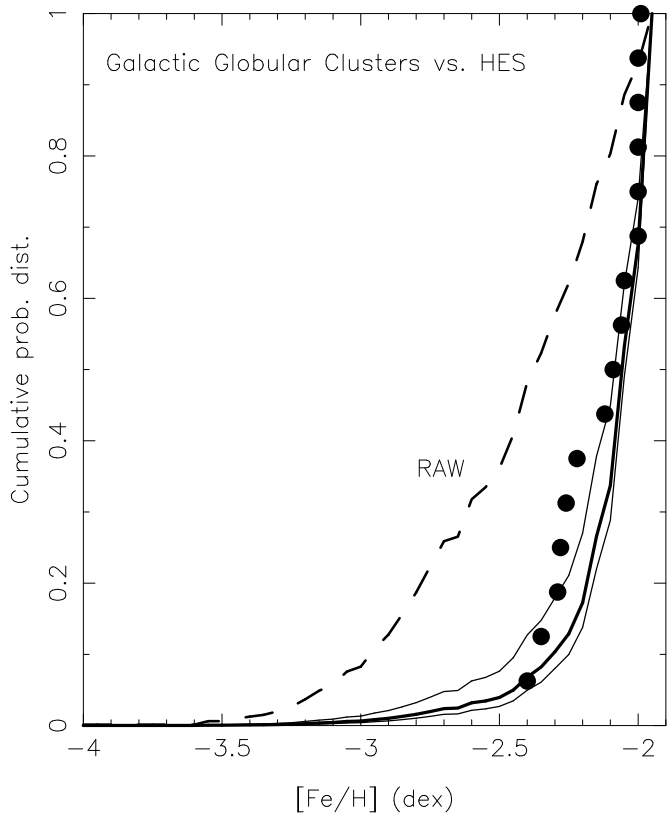

Fig. 17. Cumulative MDF for [Fe/H] < −2.0 as observed in the HES (dashed line), and with corrections for the HES selection efficiency applied (solid lines). Three different ways of applying the corrections are shown to illustrate their uncertainty: Multiplication of the observed metal-poor star counts with the corrections for $(B-V)_0 = 1.0$ (upper solid line), the $(B-V)_0$ color appropriate for each individual star in the HES sample (thick, middle line), and the corrections for $(B-V)_0 = 0.5$ (lower solid line). The cumulative MDF of the GCs [Fe/H] < −1.95 is shown by filled circles. It agrees well with that of the halo field stars if the selection efficiency corrections are applied.

claim for the four systems for which they assembled the necessary data; i.e., Carina, Fornax, Sculptor and Sextans.

Abundances are now available for large samples of stars in the nearest dSph galaxies. We concentrate here on those where there is little or no evidence for recent star formation and for which suitable samples are available. There are two additional issues that arise in a comparison of the stellar population of the dSph galaxies with the Galactic halo MDF. The first is that these metallicities are derived from line indices which measure the strength of the Ca infrared triplet (CaT) in moderate-resolution spectra. The conversion from a Ca abundance to a Fe abundance is a crucial issue, since the dSph stellar population clearly shows a different trend of [Ca/Fe] versus [Fe/H] than does the Galactic halo (see, e.g., Geisler et al. 2005; or Monaco et al. 2007), with [Ca/Fe] being smaller at a given Fe-metallicity in dSph galaxies as compared to GCs and the halo field. The second is how the sample to be observed spectroscopically in the dSph is selected. If, e.g., an equal number of stars in each color bin is chosen to probe the full range of color across the upper RGB in a dSph, the sample may be biased in metallicity, because the position of the upper RGB in the color−magnitude diagram depends on [Fe/H]. Instead, a representative subset of stars reflecting the color distribution of the stars on the RGB should be chosen.

Table 5. Cumulative halo MDF for [Fe/H] < −2.0 as observed in the HES (column "Raw"), and corrected for the selection efficiency of the survey (Cols. 3–5). For details see text.

[Fe/H]	Raw	$(B-V)_0$ adopted for correction		
		star	0.5	1.0
−4.30	0.0000	0.0000	0.0000	0.00
−4.25	0.0000	0.0000	0.0000	0.00
−4.20	0.0000	0.0000	0.0000	0.00
−4.15	0.0013	0.0001	0.0003	0.00
−4.10	0.0013	0.0001	0.0003	0.00
−4.05	0.0013	0.0001	0.0003	0.00
−4.00	0.0013	0.0001	0.0003	0.00
−3.95	0.0013	0.0001	0.0003	0.00
−3.90	0.0013	0.0001	0.0003	0.00
−3.85	0.0013	0.0001	0.0003	0.00
−3.80	0.0013	0.0001	0.0003	0.00
−3.75	0.0013	0.0001	0.0003	0.00
−3.70	0.0013	0.0001	0.0003	0.00
−3.65	0.0013	0.0001	0.0003	0.00
−3.60	0.0013	0.0001	0.0003	0.00
−3.55	0.0063	0.0005	0.0014	0.00
−3.50	0.0063	0.0005	0.0014	0.00
−3.45	0.0094	0.0007	0.0022	0.00
−3.40	0.0125	0.0009	0.0029	0.00
−3.35	0.0150	0.0011	0.0035	0.00
−3.30	0.0201	0.0015	0.0046	0.00
−3.25	0.0263	0.0019	0.0060	0.00
−3.20	0.0370	0.0028	0.0085	0.00
−3.15	0.0489	0.0037	0.0112	0.00
−3.10	0.0577	0.0044	0.0132	0.00
−3.05	0.0759	0.0058	0.0174	0.00
−3.00	0.0828	0.0063	0.0190	0.00
−2.95	0.1078	0.0084	0.0250	0.01
−2.90	0.1279	0.0102	0.0298	0.01
−2.85	0.1567	0.0129	0.0369	0.01
−2.80	0.1868	0.0158	0.0445	0.01
−2.75	0.2232	0.0196	0.0543	0.01
−2.70	0.2589	0.0238	0.0646	0.02
−2.65	0.2652	0.0246	0.0665	0.02
−2.60	0.3179	0.0319	0.0838	0.02
−2.55	0.3348	0.0346	0.0901	0.02
−2.50	0.3611	0.0395	0.1010	0.03
−2.45	0.4088	0.0498	0.1242	0.03
−2.40	0.4815	0.0680	0.1650	0.05
−2.35	0.5229	0.0822	0.1927	0.06
−2.30	0.5768	0.1037	0.2354	0.08
−2.25	0.6213	0.1288	0.2756	0.10
−2.20	0.6796	0.1725	0.3413	0.14
−2.15	0.7605	0.2657	0.4522	0.22
−2.10	0.8031	0.3371	0.5226	0.29
−2.05	0.8859	0.5323	0.6851	0.49
−2.00	0.9298	0.6759	0.7922	0.64
−1.95	1.0000	1.0000	1.0000	1.00

Bearing these caveats in mind, we have constructed the cumulative MDF for several dSph galaxies. Given the larger samples of very low-metallicity stars in these galaxies as compared to the limited number of such low metallicity Galactic GCs, we have normalized the dSph MDFs to [Fe/H] = −2.3. The selection efficiency of the HES over this lower metallicity range will be higher (i.e. closer to 1.0) and not vary as much than is the case over the regime we needed to consider for the Galactic GCs. The MDFs for Draco and for Ursa Minor (top row in Fig. 18) are based on the database of Winnick (2003). She measured CaT line strengths from spectra obtained with the multi-fiber instrument Hydra at the WIYN telescope. Her

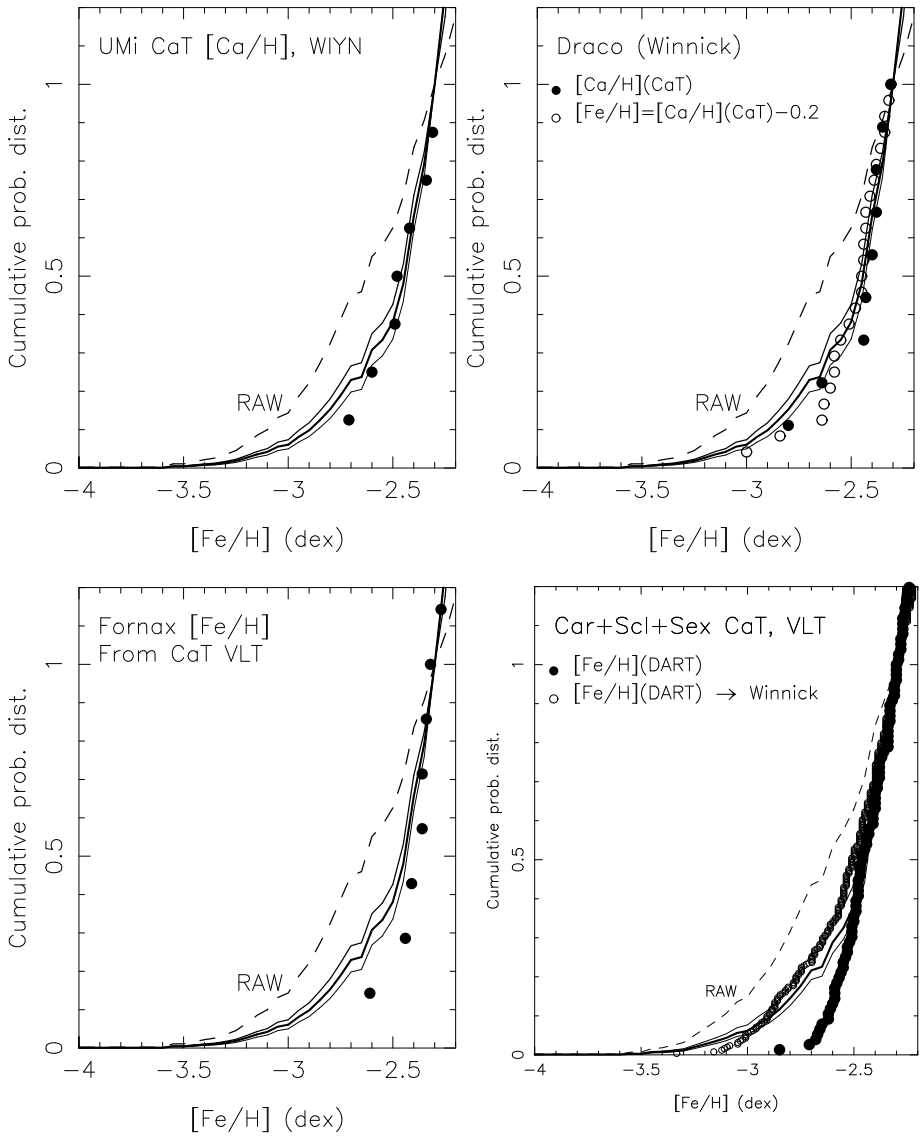

Fig. 18. Cumulative MDF for [Fe/H] < −2.3 as observed in the HES (dashed line), and with corrections for the HES selection efficiency applied (solid lines; see the caption of Fig. 17 and the text for a detailed explanation). The filled circles indicate the cumulative MDFs of Ursa Minor (*upper left*) and Draco (*upper right*), using the [Ca/H] values from Winnick (2003); for Draco we also show an estimate of the MDF for [Fe/H], assuming that [Fe/H] = [Ca/H] − 0.2 (open circles). In *the lower left panel* we show a comparison of the cumulative MDF for Fornax from Battaglia et al. (2006). In *the lower right panel* the combined cumulative MDFs of Carina, Sextans, and Sculptor based on [Fe/H] values determined in the DART project (filled circles; this data was kindly provided by the DART team) is compared to that of the HES. The result adopting the calibration of Winnick (2003) instead is shown as the open circles.

sample is selected from radial-velocity members with no metallicity bias. Winnick calibrates a relation between both [Ca/H] and [Fe/H] and CaT from observations of GC giants, making no attempt to take into account the difference in the behavior of [Ca/Fe] with [Fe/H] in these two stellar populations. We use her [Ca/H](CaT) values in the figure (solid points). The detailed abundance analyses of Cohen & Huang (2009) suggest that [Fe/H] ∼ [Ca/H](CaT, Winnick) − 0.2 for Draco giants; this yields the open circles in the Draco panel of Fig. 18. The (constant) offset arises primarily from the lower [Ca/Fe] seen among dSph giants as compared to GC giants, and includes any error in the calibration adopted by Winnick (2003). The MDF for Draco, with 24 stars at [Fe/H] < −2.3 (nine of which have [Ca/H] < −2.3), and for UMi, agree reasonably well with the halo Fe-MDF, once the selection efficiency of the HES is taken into consideration.

For the Fornax dSph we use the VLT/FLAMES+GIRAFFE survey of Battaglia et al. (2006) (their Table 4). The DART team in this paper converted their measurements of the strength of the infrared Ca triplet into Fe-metallicities (filled circles) using the relation established by Rutledge et al. (1997), which was calibrated using globular cluster giants. Battaglia advises (priv. comm.) that their sample should be unbiased with respect to metallicity. Although there are only 7 Fornax stars in the sample of Battaglia et al. (2006) with [Fe/H] < −2.3, the left panel of Fig. 18 shows that the Fornax dSph is clearly deficient in such low metallicity stars relative to the MDF of the halo field stars when the HES raw counts are used. Once the selection efficiencies are folded in, the Fornax cumulative MDF at [Fe/H] < −2.3 is much closer to that of the Galactic halo field stars as inferred from the HES.

The lower right panel of Fig. 18 shows the cumulative MDF from the combined DART sample for the Carina, Sextans, and Sculptor dSph galaxies, with [Fe/H] values kindly supplied by the DART project (filled circles). This yields a total sample of 76 stars with [Fe/H] < −2.3. Again, once the selection efficiencies are folded in, the cumulative MDF for these three dSph galaxies at [Fe/H] < −2.3 is much closer to that of the Galactic halo field stars as inferred from the HES than when the raw HES counts are used, but there still appears to be a deficit of stars in the combined dSph MDF at the lowest metallicity compared to the HES MDF.

Battaglia et al. (2008) discussed the accuracy of their conversion between Ca triplet line strength and [Fe/H], given the

difference in the behavior of [Ca/Fe] with Fe-metallicity between GCs and dSph populations. Using a comparison of high-dispersion abundance analyses with their results from CaT measurements for a limited sample of dSph giants, they conclude that their Fe-metallicities are robust to within ±0.2 dex. However, as pointed out by Cohen & Huang (2009), there are substantial differences between the calibration adopted by the VLT DART project and that of Winnick (2003), which suggest that the DART project metallicities are too high for [Fe/H] < −2.0. Hence, we converted the DART [Fe/H] values to those that would have been inferred using the CaT calibration to [Fe/H] of Winnick (2003), combining Eq. (13) of Battaglia et al. (2008) with Eq. (3.5) of Winnick (2003). The results are indicated by the open circles. The application of the CaT calibration of Winnick (2003) to the DART data produces a better agreement with the HES Galactic halo MDF. While the CaT technique appears to be valid even at [Fe/H] < −2.5 (Starkenburg 2009), the metallicity calibration needs to be improved in this [Fe/H] range. It is clear from the above that this issue is crucial in constructing a MDF. Efforts to validate and improve the calibration are currently underway by Starkenburg (2009) and others.

We thus find that the MDF of the Galactic halo field stars, as derived from the HES, agree reasonably well with that of the Galactic globular cluster system and of the stellar population of the nearest dSph satellites of the Galaxy, when the calibration for converting infrared Ca triplet line strengths into [Fe/H] of Winnick (2003) is adopted. This holds over the range [Fe/H] < −2.3, after the selection efficiency corrections to the apparent MDF from the HES have been applied. However, χ^2-tests reveal that the differences between the halo MDF and the MDFs of the GC system and the dwarf satellites are still highly significant. If the original DART calibrations and [Fe/H] are valid, adding the HES selection efficiency corrections considerably improves the agreement in deduced MDF of the dSph galaxies with the Galactic halo field stars, but still leaves a problem at the lowest metallicities.

Recently Kirby et al. (2008, 2009) developed a spectral-synthesis technique that does not use the CaT at all. They found 15 stars with [Fe/H] < −3.0 in seven of the ultra-faint dSph galaxies recently discovered by the SDSS. Since all these very low luminosity galaxies have mean [Fe/H] values of −1.9 dex or lower, this is perhaps not surprising. Cohen & Huang (2009) have obtained high resolution spectra of a sample of stars in the Draco dSph, one of the more luminous of the dSph satellites of the Galaxy, and found one star with [Fe/H] < −3.0 in that dSph, in addition to a Draco giant at [Fe/H] = −2.97 discovered earlier by Shetrone et al. (1998). In Sculptor, one star with [Fe/H] < −3.5 has recently been identified based on high-resolution spectroscopy (Frebel 2009, priv. comm.). Finally, in a sample of 16 radial velocity members of the Bootes I dSph, Norris et al. (2008) have reported a giant with [Fe/H] = −3.4, based of measurements of the Ca II K line. Follow-up, high-resolution, high signal-to-noise observations with VLT/UVES confirm the result (Norris 2009, priv. comm.). Thus, extremely metal-poor stars are present, albeit in small numbers, in both the ultra-faint and classical dSph satellites of the Galaxy.

8. Discussion and conclusions

In Sect. 6 we have shown that a reasonable agreement with the overall shape of the HES MDF can be obtained for [Fe/H] > −3.6 by most models of Galactic chemical evolution, but only the model of Salvadori et al. with $Z_{cr} = 10^{-3.4}\ Z_{\odot}$ reproduces the the sharp drop at [Fe/H] ∼ −3.6 seen in the HES MDF. The lack of stars at [Fe/H] < −3.6 is highly significant: the models typically predict that about ten such stars should be present in the HES sample, while only two are found. The significance of this discrepancy is reflected in the low probabilities for the MDFs predicted by the models and the HES MDF having the same parent distribution, as determined by KS-tests. It remains to be investigated whether the drop can be reproduced by modifying some of the assumptions of the models, or by adding further ingredients.

The HES sample discussed in this paper contains no objects with [Fe/H] < −4.2, but considering the abundance analyses of three additional stars in this metallicity range published in the recent literature, it is obvious that it exists. However, a thorough and quantitative comparison with theoretical MDFs has to await larger statistically complete and unbiased samples which include more stars with [Fe/H] < −4.0. Such samples will become available through new, deeper surveys for metal-poor stars that will commence in the near future; in particular, the Southern Sky Survey (Keller et al. 2007) and a survey to be conducted with the Chinese 4 m Large sky Area Multi-Object fiber Spectroscopic Telescope (LAMOST; Zhao et al. 2006).

In the ΛCDM picture, the Galactic halo was largely built out of disrupted satellite galaxies. If stars had already formed within them at the time of accretion, then the MDF of the Galactic halo and of the existing dSph galaxies should agree at the metal-poor end with regard to the presence of a weak tail of stars with [Fe/H] < −3.0. It is thus encouraging for the ΛCDM scenario that our analysis shows better agreement between the halo MDF and that of the dSph galaxies than claimed by Helmi et al. (2006). However, even if this were not the case, it would not necessarily be a strong contradiction to the ΛCDM scenario. According to the semi-analytical models of Salvadori et al. (2008) and Salvadori & Ferrara (2009), the MDFs of dSph galaxies can differ quite significantly from each other, depending on their individual enrichment histories. Hence their MDFs can also be different from that of the Galactic halo. An important question remaining to be answered is how the elemental-abundance ratios of the dSph stars at [Fe/H] < −3.0 compare with those of the Galactic halo stars.

Since the HES and the HK survey are in-situ surveys that predominantly sample the inner-halo population of the Galaxy (with $R < 15$ kpc), it is mandatory to consider the possibility that the (for now, poorly studied) outer-halo population of the Galaxy may indeed contain significant numbers of stars with [Fe/H] < −3.6, as might be indicated by the shift of the peak metallicity of the other-halo stars studied by Carollo et al. (2007) to [Fe/H] = −2.2, a factor of four lower than the peak metallicity of inner-halo stars. This possibility is being actively pursued by high-resolution spectroscopic follow-up of stars that are likely to be members of the outer-halo population, based on their kinematics, by a number of groups.

Acknowledgements. We thank T. Karlsson, N. Prantzos, and S. Salvadori for providing us with electronic versions of published theoretical MDFs, and for enlightening discussions. Valuable comments on an earlier version of this paper by S. Ryan are gratefully acknowledged. We thank the DART collaboration for providing us with unpublished metallicities of stars in Carina, Sextans and Sculptor. N.C. and D.R. acknowledge financial support from Deutsche Forschungsgemeinschaft through grants Ch 214/3 and Re 353/44. N.C. is also supported by the Knut and Alice Wallenberg Foundation. J.G.C. is grateful to NSF grant AST-0507219 for partial support. T.C.B. acknowledges partial funding for this work from grants AST 04-06784, AST 06-07154, AST 07-07776, PHY 02-16873, and PHY 08-226498: Physics Frontier Center/Joint Institute for Nuclear Astrophysics (JINA), all awarded by the US National Science Foundation. M.S.B. and J.E.N. acknowledge support from the Australian Research Council under grants DP0342613 and DP0663562. A.F. acknowledges support from the W. J. McDonald Fellowship of the McDonald Observatory.

P.S.B. is a Royal Swedish Academy of Sciences Research Fellow supported by a grant from the Knut and Alice Wallenberg Foundation. P.S.B. also acknowledges the support of the Swedish Research Council.

References

Allende Prieto, C. A., Sivarani, T., Beers, T., et al. 2008, AJ, 136, 2070
Aoki, W., Frebel, A., Christlieb, N., et al. 2006, ApJ, 639, 897
Barklem, P., Christlieb, N., Beers, T., et al. 2005, A&A, 439, 129
Battaglia, G., Tolstoy, E., Helmi, A., et al. 2006, A&A, 459, 423
Battaglia, G., Helmi, A., Tolstoy, E., et al. 2008, ApJ, 681, L13
Beers, T. C. 1999, in The Third Stromlo Symposium: The Galactic Halo, ed. B. Gibson, T. Axelrod, & M. Putman, ASP Conf. Ser., 165, 202
Beers, T., & Christlieb, N. 2005, ARA&A, 43, 531
Beers, T., Preston, G., & Shectman, S. 1985, AJ, 90, 2089
Beers, T. C., Preston, G. W., & Shectman, S. A. 1992, AJ, 103, 1987
Beers, T. C., Rossi, S., Norris, J. E., Ryan, S. G., & Shefler, T. 1999, AJ, 117, 981
Bessell, M., Christlieb, N., & Gustafsson, B. 2004, ApJ, 612, L61
Bond, H. E. 1981, ApJ, 248, 606
Bromm, V., & Loeb, A. 2003, Nature, 425, 812
Bromm, V., Ferrara, A., Coppi, P., & Larson, R. 2001, MNRAS, 328, 969
Carney, B., Laird, J., Latham, D., & Aguilar, L. 1996, AJ, 112, 668
Carollo, D., Beers, T., Chiba, M., et al. 2007, Nature, 450, 1020
Cayrel, R., Depagne, E., Spite, M., et al. 2004, A&A, 416, 1117
Christlieb, N., Green, P., Wisotzki, L., & Reimers, D. 2001a, A&A, 375, 366
Christlieb, N., Wisotzki, L., Reimers, D., et al. 2001b, A&A, 366, 898
Christlieb, N., Bessell, M., Beers, T., et al. 2002, Nature, 419, 904
Christlieb, N., Gustafsson, B., Korn, A., et al. 2004, ApJ, 603, 708
Christlieb, N., Timothy C. Beers, Thom, C., et al. 2005, A&A, 431, 143
Christlieb, N., Schörck, T., Frebel, A., et al. 2008, A&A, 484, 721
Clark, P., Glover, S., & Klessen, R. 2008, ApJ, 672, 757
Cohen, J., & Huang, W. 2009, ApJ, 701, 1053
Cohen, J., Christlieb, N., McWilliam, A., et al. 2004, ApJ, 612, 1107
Cohen, J., Shectman, S., Thompson, I., et al. 2005, ApJ, 633, L109
Cohen, J., McWilliam, A., Shectman, S., et al. 2006, AJ, 132, 137
Cohen, J., Christlieb, N., McWilliam, A., et al. 2008, ApJ, 672, 320
Frebel, A., Aoki, W., Christlieb, N., et al. 2005, Nature, 434, 871
Frebel, A., Christlieb, N., Norris, J., Aoki, W., & Asplund, M. 2006a, ApJ, 638, L17
Frebel, A., Christlieb, N., Norris, J., et al. 2006b, ApJ, 652, 1585
Frebel, A., Johnson, J., & Bromm, V. 2007, MNRAS, 380, L40
Geisler, D., Smith, V. V., Wallerstein, G., Gonzalez, G., & Charbonnel, C. 2005, AJ, 129, 1428
Geisler, D., Wallerstein, G., Smith, V. V., & Casetti-Dinescu, D. I. 2007, PASP, 119, 939
Gunn, J. E., Carr, M., Rockosi, C., et al. 1998, AJ, 116, 3040
Harris, W. E. 1996, AJ, 112, 1487
Hartwick, F. 1976, ApJ, 209, 418
Helmi, A., Irwin, M. J., Tolstoy, E., et al. 2006, ApJ, 651, L121
Ivezic, Z., Sesar, B., Juric, M., et al. 2008, ApJ, 684, 287
Karlsson, T. 2006, ApJ, 641, L41
Keller, S., Schmidt, B., Bessell, M., et al. 2007, PASP, 24, 1
Kim, Y., Demarque, P., Yi, S., & Alexander, D. 2002, ApJS, 143, 499
Kirby, E., Simon, J., Geha, M., Guhathakurta, P., & Frebel, A. 2008, ApJ, 685, L43
Kirby, E., Guhathakurta, P., Bolte, M., Sneden, C., & Geha, M. 2009, ApJ, submitted
Kuiper, N. 1962, in Proceedings of the Koninklijke Nederlandse Akademie van Wetenschappen, 63, 38
Lee, Y., Beers, T., Sivarani, T., et al. 2008a, AJ, 136, 2022
Lee, Y., Beers, T., Sivarani, T., et al. 2008b, AJ, 136, 2050
Lucatello, S., Beers, T., Christlieb, N., et al. 2006, ApJ, 652, L37
Monaco, L., Bellazzini, M., Bonifacio, P., et al. 2007, A&A, 464, 201
Norris, J. 1999, in The Third Stromlo Symposium: The Galactic Halo, ed. B. Gibson, T. Axelrod, & M. Putman, ASP Conf. Ser., 165, 213
Norris, J., Christlieb, N., Korn, A., et al. 2007, ApJ, 670, 774
Norris, J. E., Gilmore, G., Wyse, R. F. G., et al. 2008, ApJ, 689, L113
Omukai, K. 2000, ApJ, 534, 809
Omukai, K., Tsuribe, T., Schneider, R., & Ferrara, A. 2005, ApJ, 626, 627
Prantzos, N. 2003, A&A, 404, 211
Prantzos, N. 2007, in Chemodynamics: from first stars to local galaxies, ed. E. Emsellem, H. Wozniak, G. Massacrier, J.-F. Gonzalez, J. Devriendt, & N. Champavert, EAS Publ. Ser., 24, 3
Press, W. H., et al. 1992, Numerical Recipes in C, 2nd edn. (Cambridge: Cambridge University Press)
Reimers, D. 1990, The Messenger, 60, 13
Rutledge, G. A., Hesser, J. E., Stetson, P. B., et al. 1997, PASP, 109, 883
Ryan, S., & Norris, J. 1991, AJ, 101, 1865
Salvadori, S., & Ferrara, A. 2009, MNRAS, 395, L6
Salvadori, S., Schneider, R., & Ferrara, A. 2007, MNRAS, 381, 647
Salvadori, S., Ferrara, A., & Schneider, R. 2008, MNRAS, 386, 348
Santoro, F., & Shull, J. M. 2006, ApJ, 643, 26
Schlegel, D., Finkbeiner, D., & Davis, M. 1998, ApJ, 500, 525
Schneider, R., Ferrara, A., Natarajan, P., & Omukai, K. 2002, ApJ, 571, 30
Schneider, R., Ferrara, A., Salvaterra, R., Omukai, K., & Bromm, V. 2003, Nature, 422, 869
Schneider, R., Omukai, K., Inoue, A. K., & Ferrara, A. 2006, MNRAS, 369, 1437
Searle, L., & Sargent, W. 1972, ApJ, 173, 25
Shetrone, M., Bolte, M., & Stetson, P. 1998, AJ, 115, 1888
Starkenburg, E. 2009, in Chemical Evolution of Dwarf Galaxies and Stellar Clusters, ed. F. Primas, & A. Weiss, MPA/ESO/MPE/USM Garching Astronomy Conferences, MPA/ESO/MPE/USM (Garching: ESO)
Tsuribe, T., & Omukai, K. 2006, ApJ, 642, L61
Tumlinson, J. 2006, ApJ, 641, 1
Umeda, H., & Nomoto, K. 2003, Nature, 422, 871
Winnick, R. A. 2003, Ph.D. Thesis, Yale University
Wisotzki, L., Köhler, T., Groote, D., & Reimers, D. 1996, A&AS, 115, 227
Wisotzki, L., Christlieb, N., Bade, N., et al. 2000, A&A, 358, 77
York, D., Adelman, J., Anderson, J., et al. 2000, AJ, 120, 1579
Zhao, G., Chen, Y., Shi, J., et al. 2006, ChJAA, 6, 265

[1] Hamburger Sternwarte, Universität Hamburg, Gojenbergsweg 112, 21029 Hamburg, Germany
e-mail: [tschoerck;fzickgraf;dreimers]@hs.uni-hamburg.de
[2] Zentrum für Astronomie der Universität Heidelberg, Landessternwarte, Königstuhl 12, 69117 Heidelberg, Germany
e-mail: N.Christlieb@lsw.uni-heidelberg.de
[3] Department of Physics and Astronomy, Uppsala University, Box 515, 75120 Uppsala, Sweden
e-mail: [barklem;be]@fysast.uu.se
[4] Palomar Observatory, Mail Code 105-24, California Institute of Technology, Pasadena, CA 91125, USA
e-mail: jlc@astro.caltech.edu
[5] Department of Physics and Astronomy, and JINA: Joint Institute for Nuclear Astrophysics, Michigan State University, E. Lansing, MI 48824, USA
e-mail: beers@pa.msu.edu
[6] Carnegie Observatories of Washington, 813 Santa Barbara Street, Pasadena, CA 91101, USA
e-mail: [shec;ian;andy]@ociw.edu
[7] Research School of Astronomy and Astrophysics, Australian National University, Cotter Road, Weston, ACT 2611, Australia
e-mail: [bessell;jen]@mso.anu.edu.au
[8] Centro de Astrofisica da Univ. Porto, Rua das Estrelas, 4150-762 Porto, Portugal
e-mail: jorge@astro.up.pt
[9] IPAC, Mail Code 100-22, California Institute of Technology, Pasadena, CA 91125, USA
e-mail: solange@ipac.caltech.edu
[10] Anglo-Australian Observatory; PO Box 296, Epping, NSW 1710, Australia
e-mail: [dmj;cpc;mh;ksr;fgw]@aao.gov.au
[11] MPI for Gravitational Physics, Albert-Einstein-Institute, Am Mühlenberg, 14476 Golm, Germany
e-mail: Berit.Behnke@aei.mpg.de
[12] Universität Potsdam, Institut für Physik und Astronomie, Karl-Liebknecht-Straße 24/25, 14476 Potsdam, Germany
e-mail: cfech@astro.physik.uni-potsdam.de
[13] McDonald Observatory, The University of Texas at Austin, 1 University Station, C1400, Austin, TX 78712-0259, USA
e-mail: anna@astro.as.utexas.edu
[14] Astrophysical Institute Postsdam, An der Sternwarte 16, 14482 Potsdam, Germany
e-mail: lutz@aip.de